

**EXPERIMENTAL STUDY OF IN SITU COMBUSTION WITH DECALIN AND
METALLIC CATALYST**

A Thesis

by

DAUREN MATESHOV

Submitted to the Office of Graduate Studies of
Texas A&M University
in partial fulfillment of the requirements for the degree of

MASTER OF SCIENCE

December 2010

Major Subject: Petroleum Engineering

**EXPERIMENTAL STUDY OF IN SITU COMBUSTION WITH DECALIN AND
METALLIC CATALYST**

A Thesis

by

DAUREN MATESHOV

Submitted to the Office of Graduate Studies of
Texas A&M University
in partial fulfillment of the requirements for the degree of

MASTER OF SCIENCE

Approved by:

Chair of Committee,
Committee Members,

Head of Department,

Daulat D. Mamora
Jerome Schubert
Yuefeng Sun
Stephen A. Holditch

December 2010

Major Subject: Petroleum Engineering

ABSTRACT

Experimental Study of In Situ Combustion with

Decalin and Metallic Catalyst. (December 2010)

Dauren Mateshov, B.S., Kazakh-British Technical University

Chair of Advisory Committee: Dr. Daulat D. Mamora

Using a hydrogen donor and a catalyst for upgrading and increasing oil recovery during in situ combustion is a known and proven technique. Based on research conducted on this process, it is clear that widespread practice in industry is the usage of tetralin as a hydrogen donor. The objective of the study is to find a cheaper hydrogen donor with better or the same upgrading performance. Decalin ($C_{10}H_{18}$) is used in this research as a hydrogen donor. The experiments have been carried out using field oil and water saturations, field porosity and crushed core for porous medium.

Four in situ combustion runs were performed with Gulf of Mexico heavy oil, and three of them were successful. The first run was a control run without any additives to create a base for comparison. The next two runs were made with premixed decalin (5% by oil weight) and organometallic catalyst (750 ppm). The following conditions were kept constant during all experimental runs: air injection rate at 3.1 L/min and combustion tube outlet pressure at 300 psig. Analysis of the performance of decalin as a hydrogen donor in in-situ combustion included comparison of results with an experiment where tetralin was used. Data from experiments of Palmer (Palmer-Ikuku, 2009) was used for this purpose, where the same oil, catalyst and conditions were used.

Results of experiments using decalin showed better quality of produced oil, higher recovery factor, faster combustion front movement and higher temperatures of oxidation. API gravity of oil in a run with decalin is higher by 4 points compared to a base run and increased 5 points compared to original oil. Oil production increased by 7% of OOIP in comparison with base run and was 2% higher than the experiment with tetralin. The time required for the combustion front to reach bottom flange decreased 1.6 times compared to the base run. The experiments showed that decalin and organometallic catalysts perform successfully in in situ combustion, and decalin is a worthy replacement for tetralin.

DEDICATION

I would like to dedicate this thesis to my parents and my siblings who have always given me strength to achieve my goals.

ACKNOWLEDGEMENTS

I would like to express my gratitude and respect to my advisor, Dr. Daulat D. Mamora, for his support and advice through studying at Texas A&M University. I would like to thank my committee members, Dr. J. Schubert and Dr. Y. Sun, for serving on my committee. I would also like to thank Dr. Marco Ramirez and Dr. Persi Schacht for assistance and consultations on research.

I would also like to thank my friends and colleagues and the department's faculty and staff for making my time at Texas A&M University a great experience.

TABLE OF CONTENTS

	Page
ABSTRACT	iii
DEDICATION	v
ACKNOWLEDGEMENTS	vi
TABLE OF CONTENTS	vii
LIST OF FIGURES	ix
LIST OF TABLES	xii
1 INTRODUCTION	1
1.1 Overview	1
1.2 Research objectives	5
2 LITERATURE REVIEW	7
3 EXPERIMENTAL APPARATUS AND PROCEDURE	12
3.1 Experimental apparatus	12
3.1.1 Gas injection system	12
3.1.1.1 Nitrogen injection	12
3.1.1.2 Air injection	12
3.1.2 Combustion tube	13
3.1.3 Fluid production system	16
3.1.4 Gas chromatograph and wet test meter system	25
3.1.5 Data measurement and recording system	25
3.2 Experimental procedure	31
4 EXPERIMENTAL RESULTS	35

	Page
4.1 Overview	35
4.2 Combustion run 1 – base run.....	37
4.3 Combustion run 2 - decalin and catalyst	46
4.4 Combustion run 3 - decalin and catalyst	54
4.5 Comparison and discussion of results	62
5 SUMMARY, CONCLUSIONS, AND RECOMMENDATIONS	68
5.1 Summary	68
5.2 Conclusions	68
5.3 Recommendations	70
REFERENCES	72
VITA.....	74

LIST OF FIGURES

	Page
Fig. 1.1 - Schematic diagram of dry, forward in-situ combustion.....	3
Fig. 3.1 - Schematic diagram of experimental apparatus.....	14
Fig. 3.2 - Combustion tube.....	17
Fig. 3.3 - Dual-thermowell assembly.....	18
Fig. 3.4 - Vacuum jacket.....	19
Fig. 3.5 - Thermocouple sheaths.....	20
Fig. 3.6 - Backpressure regulator.....	21
Fig. 3.7 - Two-stage separator system.....	22
Fig. 3.8 - Condenser unit.....	23
Fig. 3.9 - Acid scrubber and drierite columns.....	24
Fig. 3.10 - Wet test meter.....	26
Fig. 3.11 - HP 5890 Series II gas chromatograph.....	27
Fig. 3.12 - Data logger unit and PC.....	28
Fig. 3.13 - Complete view of apparatus.....	29
Fig. 3.14 - Hobart A200 electric mixer.....	30
Fig. 4.1 - Produced gas composition for run no. 1 (base run).....	38
Fig. 4.2 - Gas composition and temperature profile for run no. 1 (base run).....	38
Fig. 4.3 - Apparent H/C ratio and m-ratio for run no. 1 (base run).....	39
Fig. 4.4 - Temperature profiles for run no. 1 (base run).....	40
Fig. 4.5 - Combustion front velocity for run no. 1 (base run).....	41
Fig. 4.6 - Temperature profile from fixed thermocouples for run no. 1 (base run).....	41

Fig. 4.7 - Injection and production pressures and air flow rate for run no. 1.....	42
Fig. 4.8 - Cumulative fluid production for run no. 1 (base run).....	44
Fig. 4.9 - Cumulative produced gas volume and produced gas rates for run no. 1.....	44
Fig. 4.10 - Produced oil gravity and viscosity for run no. 1 (base run).	45
Fig. 4.11 - Produced gas composition for run no. 2.....	47
Fig. 4.12 - Apparent H/C ratio and m-ratio for run no. 2.....	47
Fig. 4.13 - Temperature profiles for run no. 2.....	49
Fig. 4.14 - Combustion front velocity for run no. 2.....	49
Fig. 4.15 - Temperature profile from fixed thermocouples for run no. 2.....	50
Fig. 4.16 - Injection and production pressures and air flow rate for run no. 2.....	51
Fig. 4.17 - Cumulative fluid production for run no. 2.....	52
Fig. 4.18 - Cumulative produced gas volume and produced gas rates for run no. 2.....	52
Fig. 4.19 - Produced oil gravity and viscosity for run no. 2.....	53
Fig. 4.20 - Produced gas composition for run no. 3.....	55
Fig. 4.21 - Apparent H/C ratio and m-ratio for run no. 3.....	55
Fig. 4.22 - Temperature profiles for run no. 3.....	56
Fig. 4.23 - Combustion front velocity for run no. 3.....	57
Fig. 4.24 - Temperature profile from fixed thermocouples for run no. 3.....	58
Fig. 4.25 - Injection and production pressures and air flow rate for run no. 3.....	58
Fig. 4.26 - Cumulative fluid production for run no. 3.....	59
Fig. 4.27 - Cumulative produced gas volume and produced gas rates for run no. 3.....	60
Fig. 4.28 - Produced oil gravity and viscosity for run no. 3.....	61

	Page
Fig. 4.29 - Recovery factors for all runs.	63
Fig. 4.30 - Recovery factors for runs with decalin and tetralin.....	63
Fig. 4.31 - Cumulative oil production for runs with decalin and tetralin.....	64
Fig. 4.32 - Produced oil gravity for all runs.	65
Fig. 4.33 - Combustion front temperatures for all runs.....	66

LIST OF TABLES

	Page
Table 4.1 - Sand pack mixture properties.....	36
Table 4.2 - Flue gas composition and properties.....	39
Table 4.3 - Flue gas composition and properties.....	46
Table 4.4 - Flue gas composition and properties.....	54
Table 4.5 - Summary of experimental result.....	67

1 INTRODUCTION

1.1 Overview

The focus of industry is turning to unconventional resources with increasing demand for oil, and declining production from conventional sources. Heavy oil is part of the unconventional resources, which also includes tight gas, coalbed methane, shales and gas hydrates. Heavy oil promises to play a major role in the future of the oil industry and many countries are looking for ways to increase their production from heavy oil sources, investing in new technologies and testing them. Heavy oil and extraheavy oil make up about 40% of the world's total oil resources of 9-13 trillion bbl.(Alboudwarej H, 2006)

Heavy oil is specified as dark black, highly viscous liquid (greater than 1000 cp) with low API gravity (less than 20°API). It has low hydrogen to carbon ratio along with a high amount of carbon residues, asphaltenes, heavy metals and sulfur.

High viscosity creates difficulties with production, transportation and processing of heavy oils. All these difficulties decrease profitability of production from heavy oil reservoirs. As viscosity of crude is extremely temperature dependent, thermal recovery methods should be implemented to produce from such reservoirs. Thermal recovery methods are techniques where you introduce heat into a reservoir and include Hot Water injection, Steam Flooding, Steam Assisted Gravity Drainage (SAGD), Cyclic Steam Injection and In-Situ combustion. In steam flooding process steam is generated on surface while in in-situ combustion it is generated inside the reservoir from combustion and formation water.

In-situ combustion is one of the first thermal Enhanced Oil Recovery (EOR) processes developed. Laboratory experiments with combustion tube were performed in 1947. The method involves ignition in the reservoir and injection of air to support a firefront moving to production well. Small amount of in-situ oil is burned during combustion.

The main advantage of in-situ combustion is that the heat is created inside the reservoir, so there is no heat loss from the wellbore. This feature makes possible in-situ combustion in deep reservoirs where steam condenses to hot water due to wellbore heat loss. Heat of the steam can be lost not only from the wellbore, but to overburden and underburden of reservoir as well. This effect creates problem with steam flooding in thin reservoirs, because most of the heat is simply conducted to bordering formation near the injection well. So, thin reservoir makes in-situ combustion the preferred thermal EOR method. Producing steam requires a large amount of energy, which can be saved if in situ combustion is used where fuel for combustion is the heavy fractions of oil in the reservoir. In-situ combustion has less environmental impact because combustion takes place inside the reservoir and the process requires less equipment, so smaller is the footprint on surface.

In-situ combustion however has disadvantages compared to other thermal EOR methods. The most important of them is a safety issue. The problem is that it's impossible to control the process which is exaggerated by the high temperatures and chemical reactions occurring within the reservoir and inside the wells. Combustion front tends to move more unpredictably than steam fronts, and it is harder to get an even sweep of the reservoir. Another problem is corrosion inside production and injection wells due

to high concentration of carbon dioxide in flue gas and poorly dehydrated injection gas. Combustion process is very dependent on continuous air supply, if there is a problem with compressors combustion front dies due to lack of air.

Dry, forward combustion is a most commonly used type of in situ combustion. During this process air is injected into reservoir through injection well and oil formation is ignited. Resulting combustion front moves away from injection well. The heat generated at the combustion front propagates through the reservoir towards the production well by conduction and convection. As the combustion front moves, the oil viscosity is reduced, and thereby the oil production rate and recovery is increased. Schematic diagram illustrating dry, forward combustion is given in **Fig 1.1**.

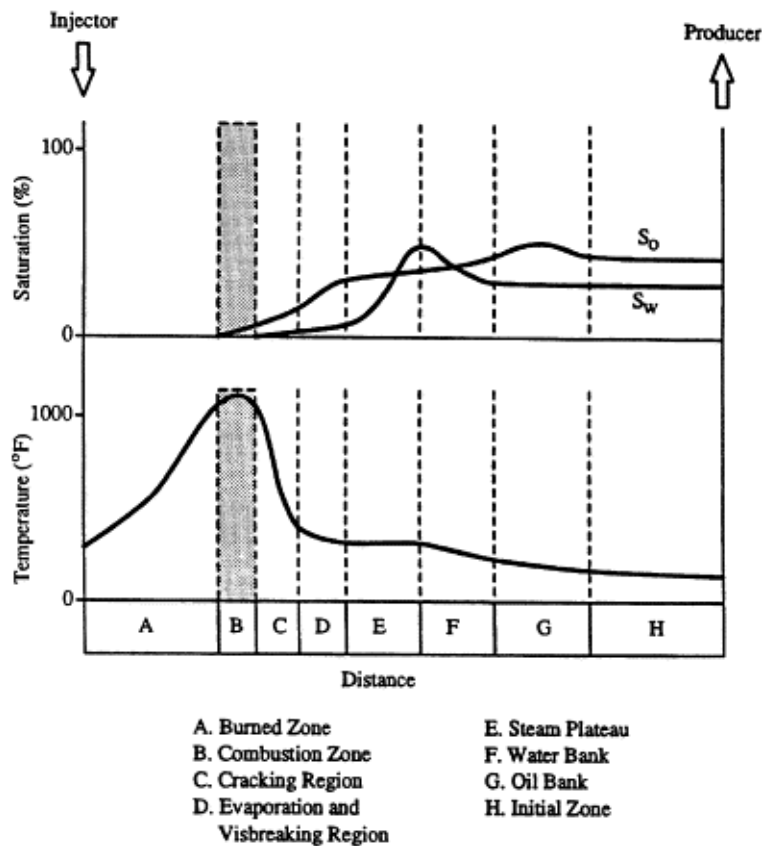


Fig. 1.1 - Schematic diagram of dry, forward in-situ combustion (Wu and Fulton, 1971).

Another type of combustion is wet combustion, where water and air are injected simultaneously or alternately. The heat in this method is transported from the burned zone to colder regions ahead by water. Water moving through the burned and combustion zones absorbs heat and turns into steam during this process and starts releasing heat after passing combustion front, where it starts condensing back into water. This method is suitable for thin reservoirs where heat loss to the adjacent formation is significant compared to that contained in the reservoir.

Next type of in situ combustion is reverse combustion, where combustion front moves from production well to injection well. Combustion is initialized in production well and combustion front moves countercurrent to the air. The oil in this method flows through the combustion front, and since the oil bank is not formed, production decreases with time. This method is unstable and has a high probability for spontaneous ignition near the injector.

Another type of combustion is quite new and called Toe-to-Heel Air Injection (THAI). One horizontal producing well and one vertical injection well is used in this method. The reservoir is ignited in the vertical well and the combustion front moves along horizontal part of the production well. Heated oil and with reduced viscosity drains to production well by gravity force.

Catalysts have been used in refineries for a long time as supporting agents to upgrade the oil in processes such as hydro-cracking and hydro-treating. The final product of these processes is lighter oil with a higher value. Studies investigating in-situ heavy oil upgrading by using catalysts or metallic additives showed modification of the reaction kinetics in a favorable way: increasing temperature of combustion, greater oxygen

consumption, more complete oxidation and more uniform combustion. Previous works show upgrading of heavy oil by application of thermal and catalytic hydro-cracking. Thermal hydro-cracking results in a significant increase in API gravity of the heavy oil produced, including an undesirable high coke formation (25 wt%), and a decreasing content of contaminations. The catalytic hydrocracking showed not only an increase of API gravity, but also a better product quality, because of its decreasing content of coke, sulfur, and metal compounds (Nares et al., 2007).

Using a combination of organometallic catalyst and decalin can improve performance of in-situ combustion. Catalysts in here will increase the quality of hydro-cracking while decalin works as a donor of hydrogen to increase the quality of oil by increasing the hydrogen-to-carbon ratio.

1.2 Research objectives

The main objective of my research is to experimentally evaluate in situ oil upgrading and increase in oil recovery by using hydrogen donor (Decalin) and an organometallic catalyst in in-situ combustion. 10° API Gulf of Mexico heavy oil is used for the experiments. For hydrogen donor I used 98% mixture of cis and trans Decahydronaphtalene (Decalin ($C_{10}H_{18}$)) and for catalyst homogenous organometallic iron acetyl acetonate ($Fe(III)(acac)_3$).

To achieve these objectives, the following tasks are performed:

- Experimentally quantify increase in cumulative oil recovery with catalyst and hydrogen donor mixed with the oil compared to in situ combustion without additives to the oil.

- Analyze influence of hydrogen donor and catalyst in upgrading of produced crude oil by comparing densities and viscosities with that of the original oil.

To achieve research objective I have conducted the following experiments:

1. One base run (original heavy oil from Gulf of Mexico, 10° API gravity)
2. Two runs with a mixture of heavy oil, decalin and metallic catalyst

The extent of upgrading will be evaluated through various analyses of the produced and initial crude oil. Following measurements will be included in these analyses:

- Cumulative oil recovered
- Produced oil API gravity
- Produced oil viscosity
- Flue gas composition
- H-C ratio and m-ratio
- Temperature profile of combustion
- Combustion front velocity
- Injection/production rates and pressures

All these measurements will help in analyzing effectiveness of decalin and catalyst on in-situ upgrading and lead to appropriate conclusion.

2 LITERATURE REVIEW

Many experimental studies have been performed to improve the in-situ combustion process. Adding different types of hydrogen donors and catalysts to upgrade heavy oil in-situ have been investigated. In this section, reviews of some of these studies are presented.

Ovalles *et al.* (2003) studied downhole heavy oil upgrading by using hydrogen donors –tetralin and methane injected with steam. Natural formation was used as a catalyst in these experiments. Experiments used Hamaca oil sands with water, tetralin and pressurized with methane in a batch reactor. Each experiment took at least 24 hours at 280-315°C and 1600 psi pressure. Laboratory experiments showed 4° increase in the API gravity (from 9 to 12°) of the upgraded product, a two-fold reduction in the viscosity and approximately 8% decrease in asphaltene content. (Ovalles et al., 2003)

Zhong *et al.* (2003) performed experiments on aquathermolysis of Liaohe heavy oil which involved the addition of catalyst and hydrogen donors under steam injection conditions. Laboratory experiments were carried out in a reactor with the Liaohe heavy oil, distilled water, catalyst (Fe(II)) and hydrogen donor (tetralin) at different temperatures and reaction times. It was found that experiments in which only water and hydrogen donor were added showed approximately a 40% oil viscosity reduction. Addition of catalyst alone lead to 60% decrease of oil viscosity compared with the original crude oil. Combination of catalyst and hydrogen donor decreased oil viscosity further up to 90%. Molecular weight of oil, sulfur, resin and asphaltene contents were decreased, while H/C ratio, saturated and aromatic hydrocarbons content increased by adding catalyst and hydrogen donor to aquathermolysis process. Field testing of the

process using catalyst and hydrogen donor was carried out at five wells of Liaohe field and resulted in oil recovery improvement and oil upgrade. (Zhong et al., 2003)

He *et al.* (2005) proposed cation exchange of metallic salts with clay as a mechanism to create activated sites that enhance combustion reactions between oil and oxygen. This paper describes an experimental study combining tube runs that gauge combustion performance and ramped temperature oxidation tests that measure the kinetics of combustion of heavy and light oil from Cymric field. Sand and clay surfaces were examined for evidence of cation exchange and alteration of surface properties by metallic salts. Results of experiments demonstrated improved performance in all parameters including lower activation energy, greater oxygen consumption, lower temperature threshold and more complete oxidation. Introduction of water soluble catalyst (Fe^{3+}) enhanced fuel deposition for 34° API Cymric crude oil. Whereas for 12°API crude oil from Cymric, addition of catalyst enhanced HTO reactions producing more complete combustion. (He et al., 2005)

Ramirez *et al.* (2007) conducted research on in-situ combustion of Gulf of Mexico heavy oil with the use of catalysts. The catalyst, in liquid phase, is based on Molybdenum, Cobalt, Nickel and Iron and is previously mixed with crude oil with a concentration of 750 ppm wt. Two runs were done: one with catalyst and one without for comparison. Combustion tube run using catalyst showed important effects such as: production acceleration, sustained initial temperature of combustion, increase in production, higher combustion efficiency and faster combustion front. (Ramirez-Garnica et al., 2007)

Nares *et al.* (2007) investigated upgrading effects of metallic oxides on heavy crude oils during thermal hydrocracking. Gulf of Mexico heavy crude oil with 12.5°API gravity was used in the experiments. Experiments were carried out in a batch reactor with a capacity of 1800 ml. Two supported catalysts were used for upgrading: MoCoP/Al₂O₃ and MoCoNiWP/Al₂O₃. Organometallic catalysts were dissolved in a hydrogen donor (tetralin), and it was activated with the heavy oil at 543 K. This work showed upgrading of heavy oil through thermal and catalytic hydrocracking. Strong hydrogenation properties of tetralin reduce the high coke formation. Using a catalyst in hydrocracking showed not only an increase in API gravity, but also better product quality due to lower content of coke, sulfur and metal compounds. (Nares et al., 2007)

Cristofari *et al.* (2008) investigated applicability of cyclic solvent injection into heavy and viscous oil followed by in-situ combustion of heavy residues. Both solvent injection and in-situ combustion are technically effective: the solvent reduces oil viscosity in-situ and extracts the lighter crude-oil fractions, combustion cleans the near well region and stimulates thermally the oil production. Hamaca (Venezuela) and West Sak (Alaska) crude oils were employed. Pentane, decane and kerosene were used as solvents. Hamaca oil showed good burning properties, especially after pentane injection. Pentane extracted lighter components of the crude and deposited preferentially effective fuel for combustion. West Sak did not exhibit stable combustion properties without solvent injection, following solvent injection and even with added metallic additives. These experiments showed applicability of this method to the broad range of reservoirs with properties similar to Hamaca. (Cristofari et al., 2008)

Ramirez *et al.* (2008) investigated the effect of using ionic liquid base Nickel catalyst and tetralin on combustion of heavy oil. The objective of the research is to increase mobility and quality of oil inside the reservoir during the combustion. The catalyst is mixed with 12.5° API Mexican Gulf heavy crude oil with a concentration 500 ppm wt. Triturated dolomite carbonate of 40-mesh is used as the matrix in the sandmix. Two runs were done: one with catalyst and one without. Experiments in combustion tubes using this Nickel ionic solution as catalyst showed important effects as follows: production acceleration, sustained initial temperature of combustion, increase in production, enhanced oil production, higher combustion efficiency and faster combustion front. The authors came to the conclusion that using Nickel ionic solution catalyst at low concentration resulted in an increase in the oil recovery factor and oil upgrade. (Ramirez-Garnica *et al.*, 2008)

Mohammad and Mamora (2008) conducted experiments to verify the feasibility of in-situ upgrading of heavy crude oil by using a hydrogen donor (tetralin) and an organometallic catalyst, $\text{Fe}(\text{CH}_3\text{COCHCOCH}_3)_3$. Three cases were considered in experiments: pure steam injection, steam injection with tetralin and steam injection with tetralin and catalyst. The catalyst was dissolved in tetralin at a concentration of 750 ppm. Two types of runs with steam additives were conducted: additives premixed with sandmix and additives injected as a slug. The Jobo oil used had a 12.4° API gravity and viscosity of 7800 cp at 30°C. Acceleration of oil production and increased oil recovery were observed in all runs. Using tetralin alone as an additive at 5 wt% increased oil recovery by 15%. Premixed tetralin and catalyst run showed 20% increase of oil recovery. (Mohammad and Mamora, 2008)

Decalin is a hydrogen donor which has not been used in in-situ combustion. My main research objective is to investigate the upgrading abilities of decalin with a catalyst, and their applicability to Gulf of Mexico heavy oil.

3 EXPERIMENTAL APPARATUS AND PROCEDURE

3.1 Experimental apparatus

The experimental apparatus consists of five main parts: gas injection system, combustion tube, fluid production system, gas chromatograph and wet test meter system, and data logging system. Descriptions of each part of apparatus and procedures are given in this section. Schematic diagram of experimental apparatus is presented in **Fig 3.1**.

3.1.1 Gas injection system

The gas injection system consists of two parts: nitrogen injection and air injection. Both paths go through $\frac{1}{4}$ in. tubing and are independent of each other. They are opened or closed to the system by valves on the control panel. The injected air or nitrogen rate is controlled by a mass flow controller, installed before the injection pressure transducer. The $\frac{1}{4}$ in. tubing line is reduced with Swagelok fittings to $\frac{1}{8}$ in. tubing line, which is the gas inlet to the combustion tube.

3.1.1.1 Nitrogen injection

Nitrogen is used to flush the system, to remove any free oxygen from it, before any combustion run. Nitrogen is also used to pressurize the combustion tube by closing the pressure regulator at the end of the production stream. At the end of an experiment, nitrogen is injected into the system to kill the combustion and cool down the tube.

3.1.1.2 Air injection

Air is injected at a constant rate of 3 L/min throughout the combustion run. The cylinder with chromatography quality air is connected to the injection system. When the

temperature at the igniter level reaches 570°F (300°C) nitrogen injection is changed to air injection at 3 L/min flow rate. Air injection will continue until the front reaches the bottom of combustion tube. At this instance, injection is switched to nitrogen to kill the combustion and flush the combustion tube.

3.1.2 Combustion tube

The combustion tube (**Fig. 3.2**) is a stainless steel cylinder with an external diameter of 3 in. (7.62 cm), a wall thickness of 1/16 in. (0.16 cm) and a length of 40-1/8 in. (101.92 cm). Sharp-edged flanges seal the ends of the cell to copper gaskets. A 10-1/2 in long x 3/4 in. tube was silver soldered to the center of the top flange, and a 1 in. x 3/4 in. Swagelok fitting was machined and silver soldered to it. The assembly provided the path for the introduction of two 3/16 in. thermowells (**Fig. 3.3**), the one corresponding to a fixed set of thermocouples was 57-3/8 in. long, the other 56-1/2 in. long. A 10 in. long x 5/16 in. tubing was silver soldered to the bottom flange of the combustion tube to allow the collection of fluids in the production system.

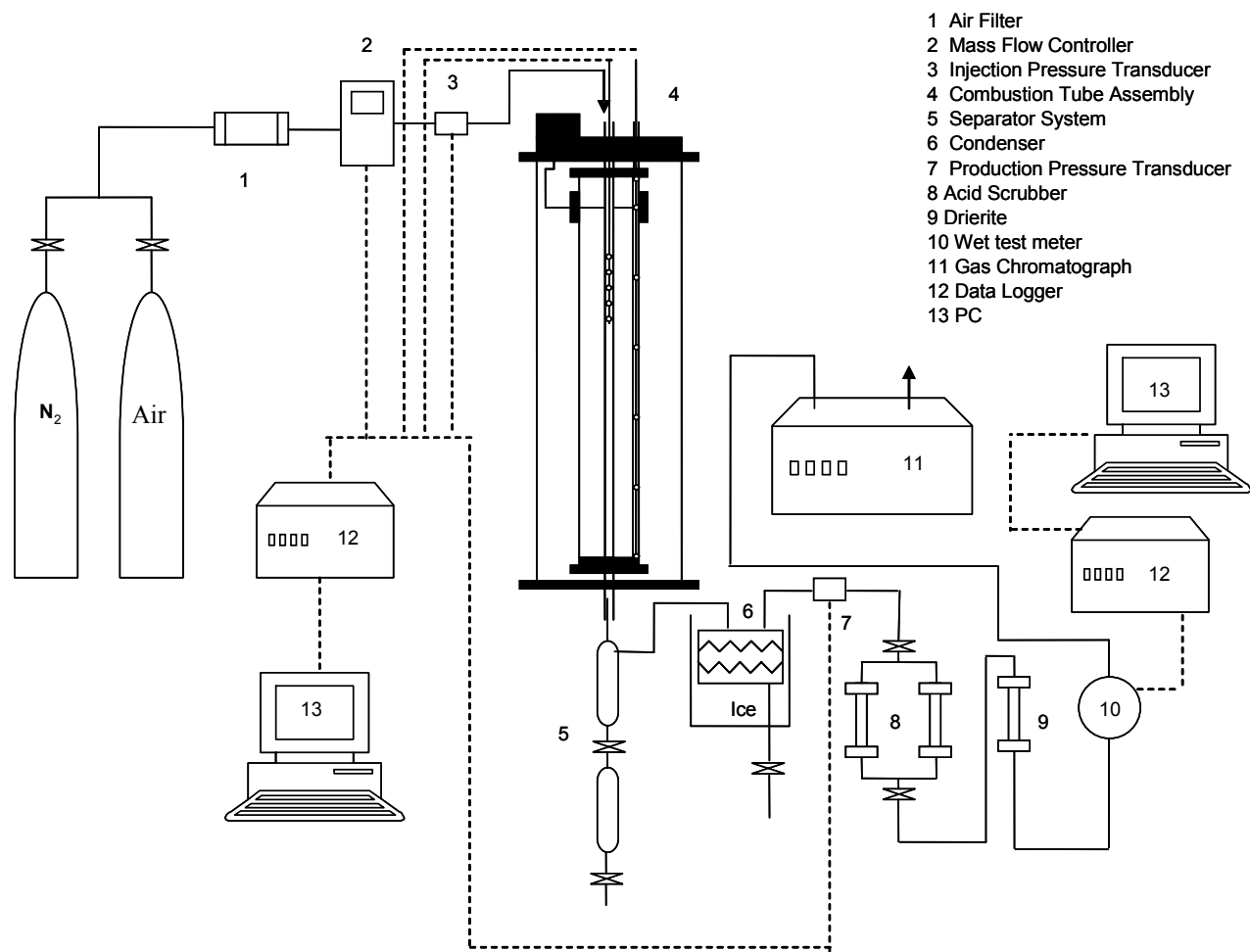


Fig. 3.1 – Schematic diagram of experimental apparatus.

The combustion tube is placed inside the vacuum jacket (**Fig. 3.4**), a 6-1/2 in. internal diameter tube (8 in. external diameter) 46 in. long. The jacket is wrapped with electric band heaters and covered with a one inch thick insulation. Flanges seal the ends of the vacuum jacket to rubber o-rings. A connection installed at the top flange of the jacket provides electric current to the resistance igniter, and drilled holes allow the insertion of the top tubing end of the combustion cell. The bottom flange also allows the insertion of the bottom end of the combustion cell and also provides a tubing connection for vacuum purposes. The vacuum jacket is isolated from the combustion cell with Teflon ferrules installed in both flange ends. The exterior of the vacuum jacket is an aluminum cover with respective aluminum end caps. The center of the jacket is connected to a swivel that allows it to be rotated from the horizontal to vertical position.

One set of eight fixed J-type thermocouples (spaced 14.1 cm apart) runs through the assigned thermowell end and a set of six movable J-type thermocouples spaced 0.5 cm apart runs through the other end. All thermocouples used are 0.002 in. diameter. The set of eight thermocouples was inserted inside a 1/8 in. diameter x 63-1/2 in. long thermocouple sheath (**Fig 3.5**) at the following depths: 1.4, 11.0, 25.1, 53.3, 67.4, 81.5, and 95.6 cm respectively measured from the top of the combustion tube. The other set of thermocouples was inserted inside a 1/8 in diameter x 62-1/8 in long thermocouple sheath (**Fig 3.5**). In this set the bottom thermocouple was set at 91.0 cm and the rest were spread 0.5 cm apart in a 2.5 cm length.

The combustion tube system is placed vertically and is secured to the production end and to the arm of the motor of the movable thermocouple set. Each one of the thermocouples is connected to its terminal to display or register its signal to the data logger and/or the control panel and/or PC monitor.

3.1.3 Fluid production system

A backpressure regulator (**Fig. 3.6**) maintains the outlet pressure of the combustion tube at a constant predetermined level during the experiment. The liquids leaving the combustion tube pass through a two-stage separator system (**Fig. 3.7**) where they are collected at the production outlet. Gases pass through a condenser unit (**Fig. 3.8**) containing ice to recover any volume of liquid in this stream. Gases flowing to the gas chromatograph are scrubbed of acid, using a column of permanganate, and dehydrated, using a column of calcium sulfite, before entering the next system (**Fig. 3.9**).



Fig. 3.2 – Combustion tube.



Fig. 3.3 – Dual-thermowell assembly.

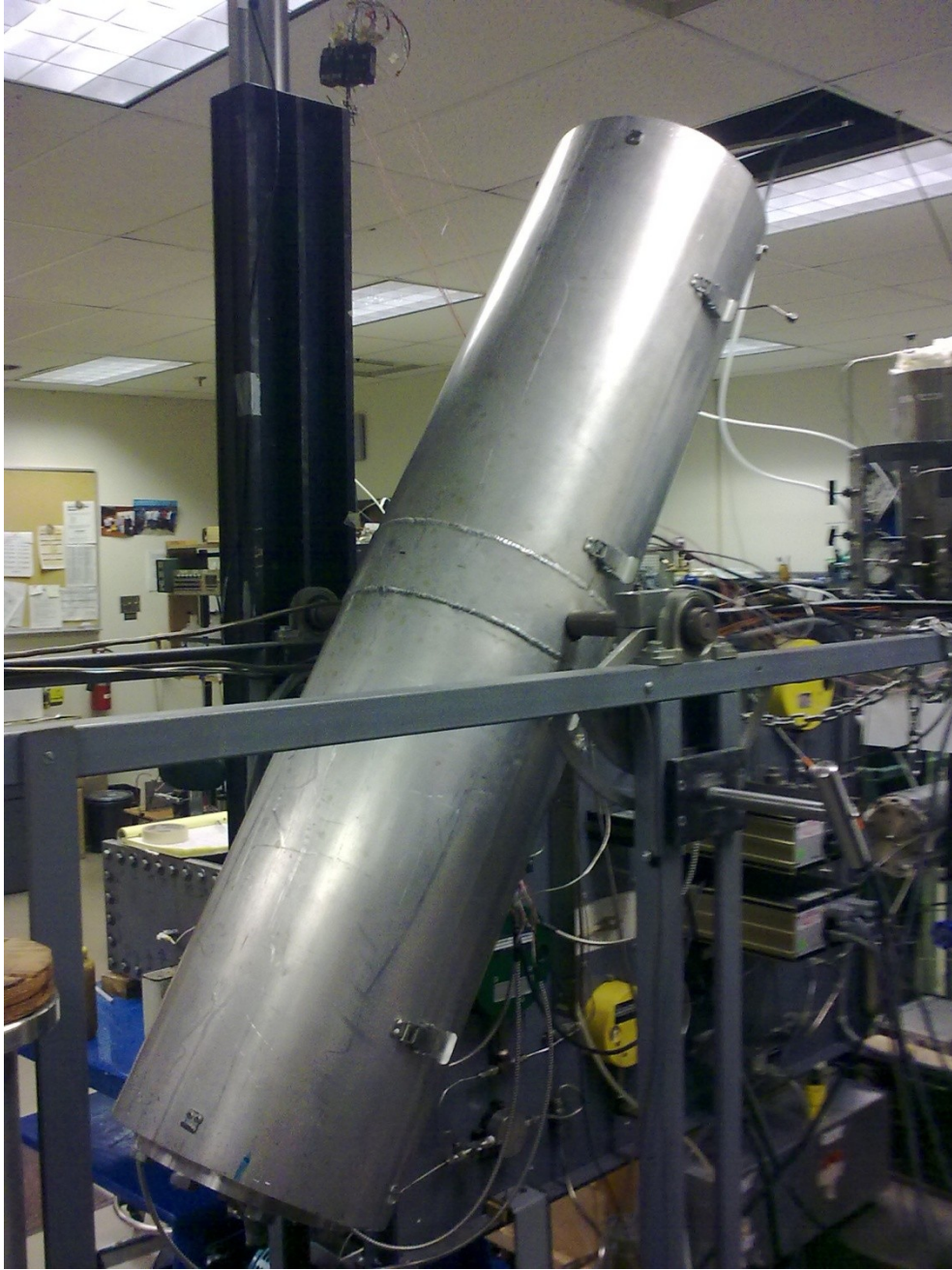


Fig. 3.4 – Vacuum jacket.

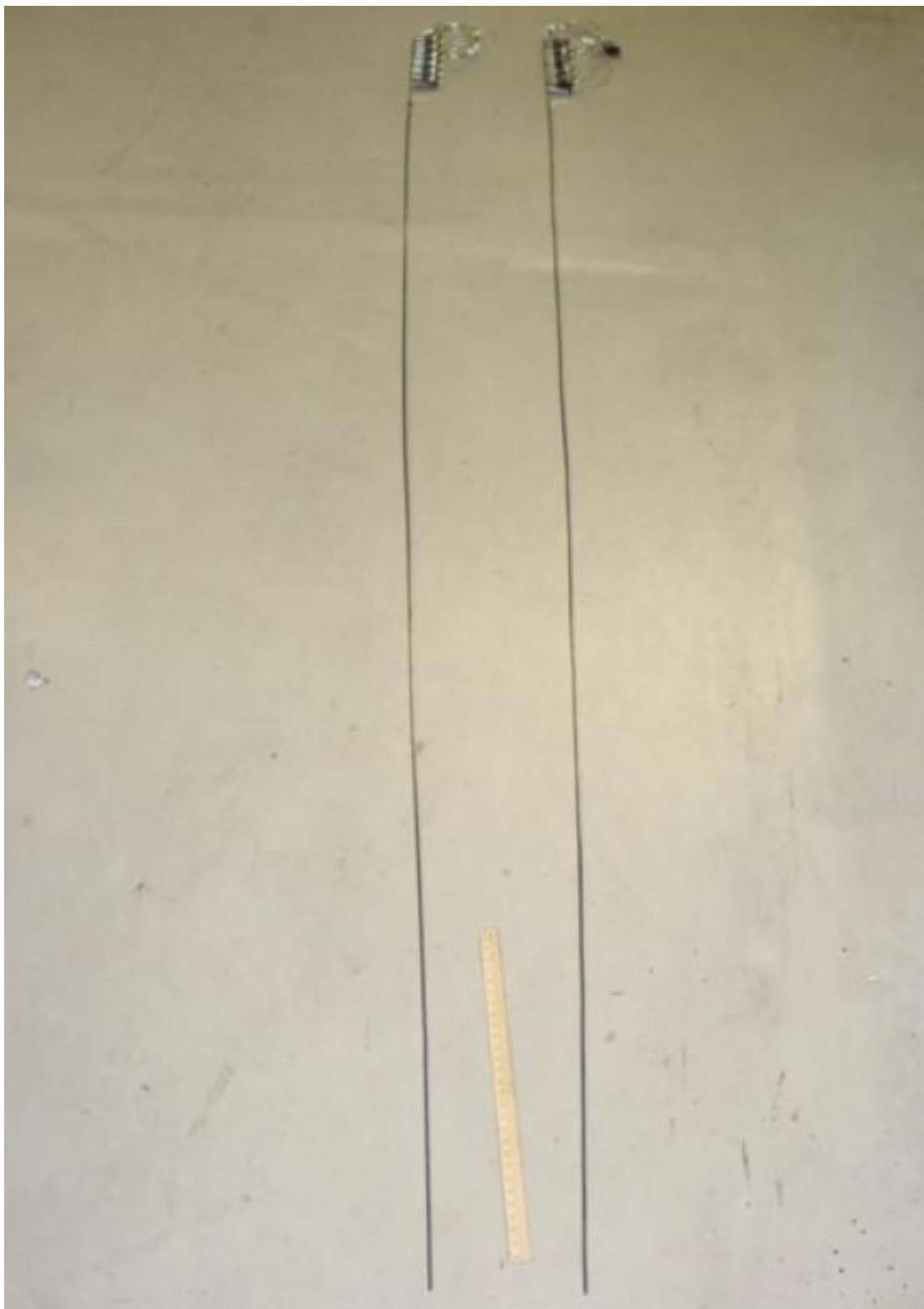


Fig. 3.5 – Thermocouple sheaths.



Fig. 3.6 – Backpressure regulator.

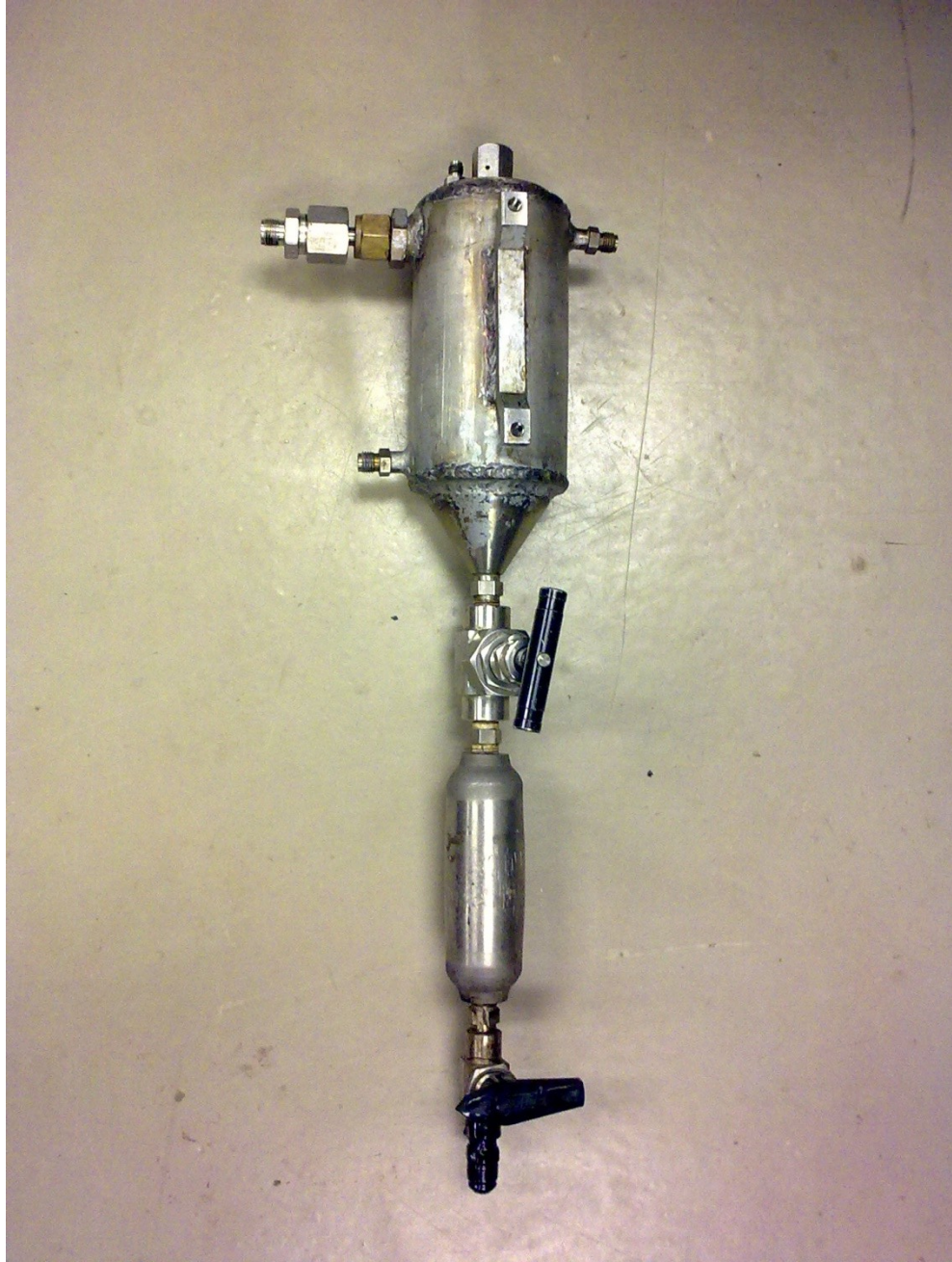


Fig. 3.7 - Two-stage separator system.



Fig. 3.8 – Condenser unit.



Fig. 3.9 – Acid scrubber and drierite columns.

3.1.4 Gas chromatograph and wet test meter system

Scrubbed and dehydrated gas flows to the wet test meter (**Fig 3.10**) where the volume of produced combustion gas is measured and recorded using the data logger/PC. A small fraction of produced gas is injected into the HP 5890 Series II gas chromatograph (**Fig. 3.11**) where the gas is analyzed for carbon dioxide, oxygen, nitrogen, and carbon monoxide about every 15 minutes. This data is registered by a HP 3966A Integrator.

3.1.5 Data measurement and recording system

Two data loggers and two personal computers (**Fig. 3.12**) are used to record the following parameters: time, jacket temperatures, fixed thermocouple temperatures, movable thermocouple temperatures, injection pressure, production pressure, depth of bottom movable thermocouple, gas injection rate, average produced gas rate, cumulative produced gas rate. The parameters are recorded at 30-second intervals and most of them are displayed on the PC monitors for monitoring purposes. A complete view of the apparatus can be seen in **Fig. 3.13**.



Fig. 3.10 – Wet test meter.



Fig. 3.11 – HP 5890 Series II gas chromatograph.



Fig. 3.12 – Data logger unit and PC.

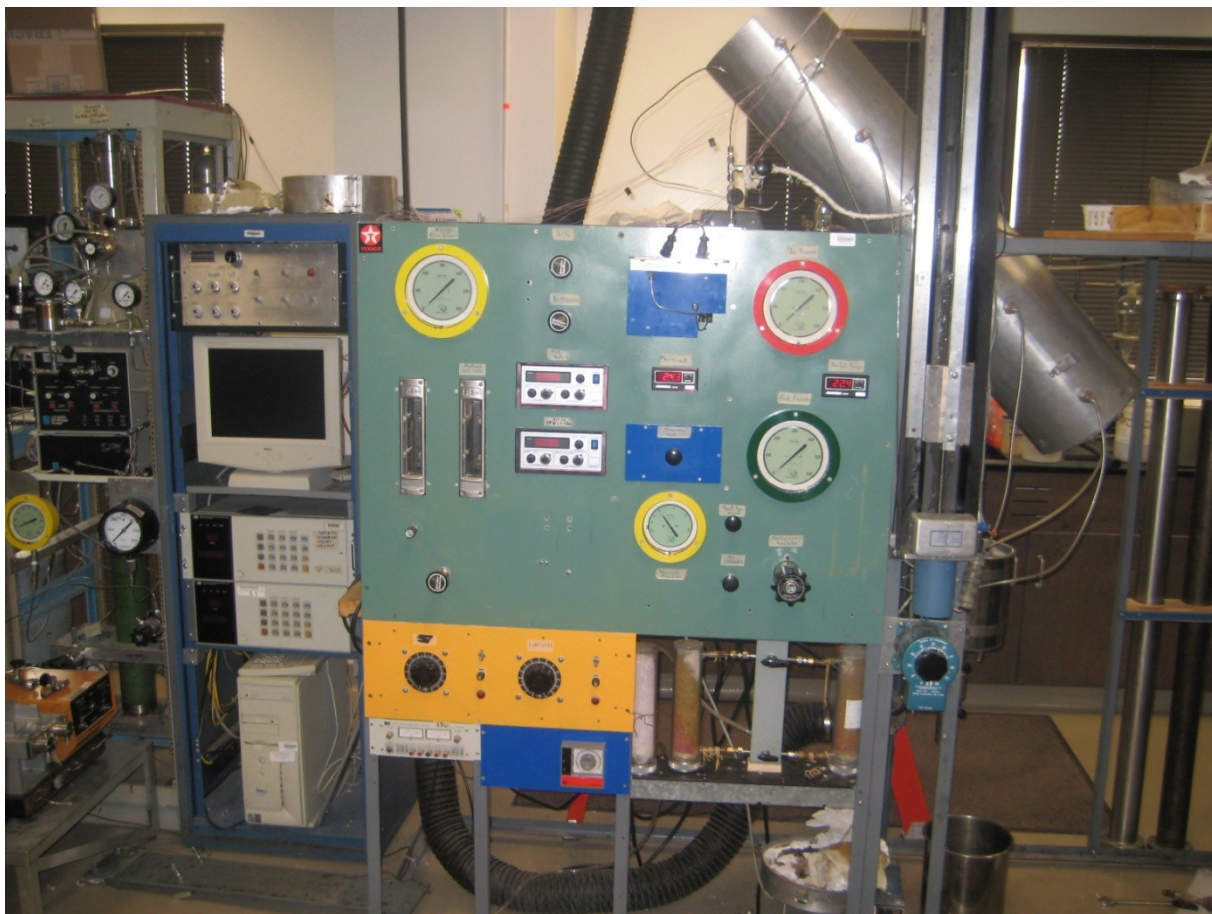


Fig. 3.13 – Complete view of apparatus.



Fig. 3.14 – Hobart A200 electric mixer.

3.2 Experimental procedure

The bottom flange of the combustion tube was installed. Two 3/16 in. thermowells connected to meshed steel screens at the bottom, to prevent sand blocking, were introduced into the tube. After this, the top flange of the combustion tube was installed and the flange bolts fastened. Then the weight of the combustion tube was weighed. After this combustion tube was filled with water. The injection assembly was installed in preparation for a pressure test of the fastenings at the bottom flange. The cell was pressure tested for leaks at 300 psig for about 20 mins. Once the pressure test was successfully completed, the pressure in the combustion tube was allowed to drop to atmospheric. After draining out the water, the top flange was removed and combustion tube is dried by injecting air.

A mixture of decalin, ferric acetylacetonate and n-butanol was prepared to be premixed with 10⁰ API Mexican Gulf heavy crude oil. Next, a mixture of carbonate rock, water and oil was made in a large mixing bowl. About 7780 g. of 40 mesh carbonate and 180 g. of water were mixed in an electric mixer until the mixture was evenly moist. The Hobart A200 electric mixer (**Fig. 3.14**) is used. Then 1315 g. of oil premixed with decalin (5% concentration by oil weight) and iron catalyst (750 ppm) were added and mixed thoroughly to obtain a uniform mixture. The final mixture was weighted to determine the loss due to mixing.

After this, portions of about 200 g. of mixture were introduced into the tube once the combustion tube was safely fastened in a vertical position. A heavy metal plunger that passed over the thermowells was used to tamp the sample into the tube. The process of adding sample and tamping was repeated until the tube was filled to about 10 cm from

the top. Top flange was installed again and the weight of the combustion tube filled with mixture was weighed and compared to the weight of the empty tube earlier measured to determine the amount of mixture in the combustion tube. Top flange was uninstalled again and about 5 ml of linseed oil was placed on the top of the sample to accelerate ignition. The combustion tube was then filled to the top with clean 100-mesh sand. The pure sand acts as an air diffuser for uniform air injection into the sandmix.

The top flange of the combustion tube was installed and the flange bolts fastened. A pressure test was performed on tamping site to check the fastening on top flange. The injection assembly was carefully installed, passing through the thermowells, and Teflon ferrules passed through them and tightened. Nitrogen was introduced at the injection inlet and with the outlet of the combustion tube plugged, the cell was pressure tested for leaks at 350 psig for 20 minutes. Once the pressure test was performed successfully, the outlet plug of the combustion cell was slowly opened and the pressure in the tube is released. The injection assembly was dismantled and an electric igniter was placed and tightened at the exterior of the combustion tube at the same depth where the linseed oil was placed. The bottom flange of the combustion tube was wrapped with insulation. The tube was then placed carefully inside the vacuum jacket which was tilted to about 30° from the horizontal to allow better handling of the combustion tube. The electric igniter was connected to the ignition terminals of the top flange of the vacuum jacket and the latter was tightened. Teflon ferrules were tightened to the outlet and injection assembly to seal the vacuum jacket from the combustion tube. The injection assembly was replaced in its position and combustion tube was pressure tested to check connection of injection assembly and ferrules of thermowells. Then the fixed and movable thermocouple sheaths

were inserted in their respective thermowells. The vacuum jacket was placed in a vertical position and the outlet of the combustion tube fastened to the production section. The movable thermocouple sheath was fixed to the motor arm and all thermocouples were connected to their terminals. The vacuum jacket was tested for thirty minutes with a vacuum of about -28 inches Hg. The injection line was connected to the assembly, and the vacuum jacket heater was set to about 122°F (50°C) and left overnight to allow the temperature of the sandmix to stabilize. A band heater set at 30°C was wrapped around the separator so as to ensure unobstructed flow of produced oil through the separator into the sample bottles.

Prior to the beginning of the experimental run, the mass flow controller was calibrated to the injection rate, the gas chromatograph was also calibrated, the bottom of the movable thermocouple sheath was raised to the linseed oil depth, and the sandpack was pressurized with nitrogen to 300 psig. Electric current was gradually introduced into the igniter using a variable power transformer. Approximately 60 minutes later, the temperature in the combustion tube at the igniter level (movable thermowell placed at the linseed oil depth) reached about 570°F (300°C) and air injection was initiated at 3 L/min. The backpressure regulator was adjusted to maintain a tube outlet pressure of 300 psig. The movable thermocouple reading in the instruments panel and PC activated to record data was observed to increase rapidly to about 986°F (530°C), a clear indication that ignition occurred inside the combustion tube. Combustion gas composition was measured about every 15 minutes; temperature profiles approximately every 2 in. (5 cm), and production liquids every 10-15 minutes. Accurate readings of temperature profiles were taken with the set of six movable thermocouples, spaced 0.5 cm from each other, which

allowed the recording of 6 entries just behind and ahead of the combustion front. These entries were made by pressing the enter key on the PC component of the data logger.

Liquids were collected in graduated sample bottles which were capped for subsequent analysis. The end of the combustion run occurred when no oil production was attained, in other words, the sandpack was burned to the bottom flange of the combustion tube. Combustion runs varied between 6-10 hours.

4 EXPERIMENTAL RESULTS

4.1 Overview

For all the runs conducted in this research several experimental parameters were kept constant to allow for a valid comparison between runs. Parameters kept constant for all runs were:

- Initial cell temperature: 50°C
- Air injection rate: 3 SL/min
- Production pressure: 300 psi

Rock, water and oil weights in the sandmix were kept as constant as possible to have the same oil, water and gas saturations for a mixture. Consistent mixing and tamping process help ensure the porosity of sandmix is the same for all runs. The properties of the mixture inside the combustion tube are shown in **Table 4.1**.

In this section I will analyze each run and report summaries of them separately as a section. Comparison between all these cases will be given as a review at the end of the section. Runs that will be discussed are as follows:

Run 1: Combustion of Gulf of Mexico original heavy crude oil.

Run 2: Combustion of Gulf of Mexico heavy crude oil with decalin and iron catalyst.

Run 2: Combustion of Gulf of Mexico heavy crude oil with decalin and iron catalyst.

Table 4.1 – Sand pack mixture properties.

	Run 1	Run 2	Run 3
Weight of mixture, g	7471	7072.51	7090
Sand, g	6266.5	5932.26	5946.93
Water, g	147.12	139.28	139.62
Oil, g	1057.37	1000.97	1003.44
S _o , %	61.35	54.3	54.59
S _w , %	8.52	7.54	7.58
S _g , %	30.12	38.15	37.82
Φ, %	43.36	46.38	46.25

For each run I calculated the apparent hydrogen-carbon (H/C) ratio and m-ratio from analysis of composition of the effluent gas. If CO₂ and CO are the mole percent of carbon dioxide and carbon monoxide, respectively, in the produced gas, the m-ratio is given by Eq. 1 (Mamora and Brigham, 1995).

$$m = \frac{CO}{(CO+CO_2)} \quad (1)$$

If O_{2p} and N₂ represent the mole percent of oxygen and nitrogen in the effluent gas, then the mole percent of consumed oxygen, O_{2c}, can be calculated from a nitrogen material balance and is given in Eq. 2.

$$O_{2c} = 0.2682N_2 - O_{2p} \quad (2)$$

Based on oxygen material balance, and using Eq. 2, the apparent atomic H/C ratio is calculated (Mamora and Brigham, 1995):

$$F_{HC} = 4 \frac{0.2682N_2 - O_{2p} + CO_2 + 0.5CO}{CO_2 + CO} \quad (3)$$

It is called apparent because calculated values are not directly measured but inferred from stoichiometry. It was assumed that all of the oxygen disappearance in combustion gas is due to production of water. This is not always the case; at low temperatures (lower than 345°C) oxygen combines with the residuum as additional reactions.

4.2 Combustion run 1 – base run

From gas compositions graph (**Fig 4.1**) we can see that composition of flue gas is very inconsistent. In some parts we produce more oxygen than carbon dioxide. For some reason we don't have proper combustion. It can be that channeling was created in this segment and injected air was not used for combustion, and bypassing the flame went directly to bottom flange. So I constructed a graph with compositions of oxygen and carbon dioxide on y-axis, and temperatures of combustion front on given time versus time on the secondary y-axis (**Fig 4.2**). This graph can help understand dependence between temperature and flue gas composition. **Fig 4.2** shows the temperature is minimal at 470 minutes and is at about 330°C while the oxygen concentration reaches a maximum of about 15%. This indicates the development of low temperature oxidation (LTO). Unlike combustion which produces CO₂, CO, and H₂O as its primary reaction products, LTO yields water and oxygenated hydrocarbons, such as carboxylic acids, aldehydes, ketones, alcohols, and hydroperoxides. The resulting oxygenated oils can have significantly higher viscosities, lower volatilities, and lower gravities than the virgin oils. Compositionally, LTO has been found to increase the asphaltene content of the oil and to decrease its aromatic and resin contents. The mechanisms of LTO are extremely complex, but condensation to higher-molecular-weight material has been proposed by several researchers. (Fassihi et al., 1990)

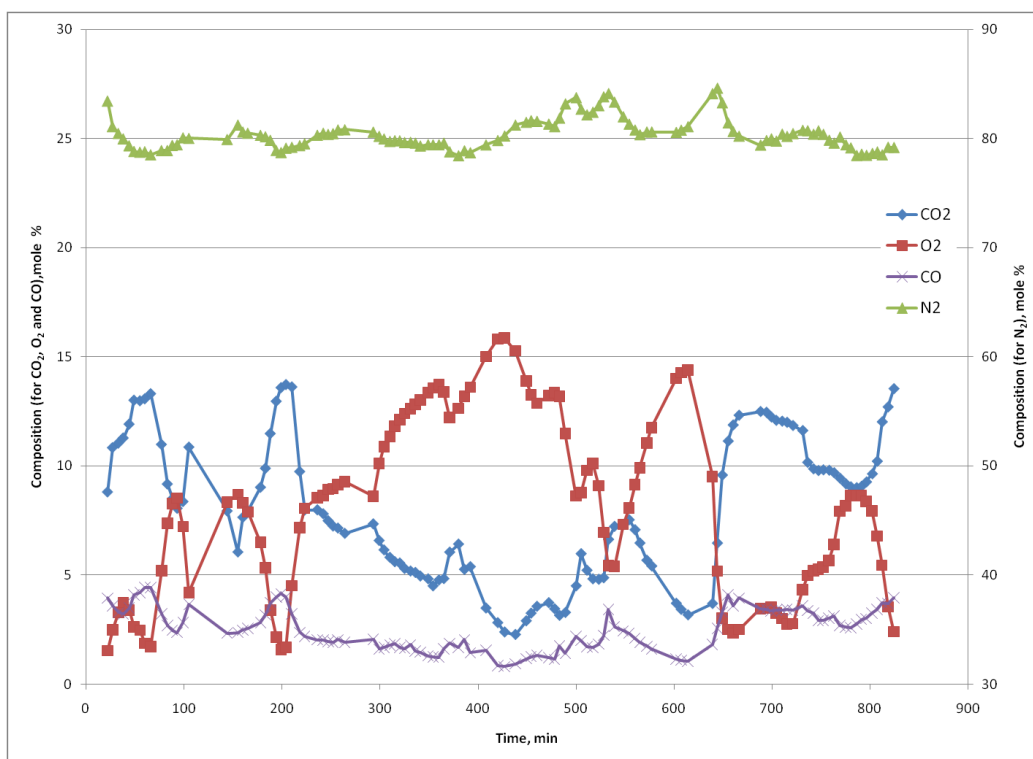


Fig. 4.1 – Produced gas composition for run no. 1 (base run).

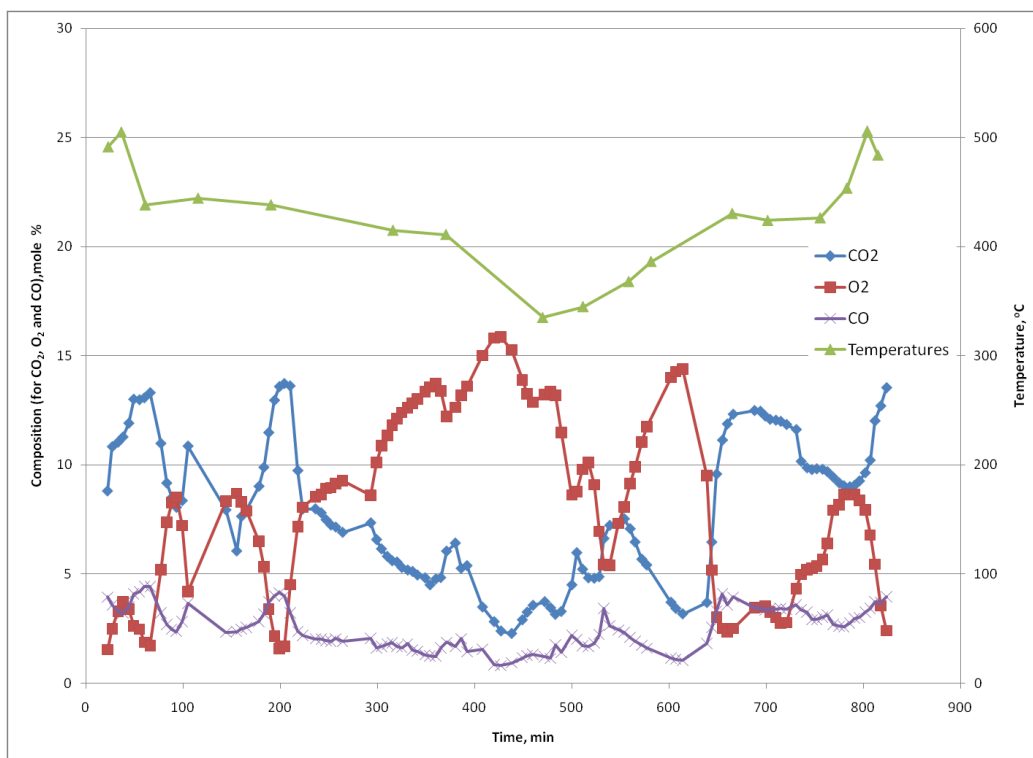


Fig. 4.2 - Gas composition and temperature profile for run no. 1 (base run).

Based on gas analysis results, apparent H/C and m-ratios were calculated as shown in **Fig 4.3**. Instability of produced gas concentrations creates big fluctuations in apparent H/C ratio. This can be explained by low temperature oxidation occurring in some segments of tube. One of the probable reasons is channeling through the center of the combustion tube. Despite this, average values of apparent H/C ratio and m- ratio are quite low. Average, median, minimal and maximum values of gas concentrations and apparent H/C and m-ratios are given in **Table 4.2**.

Table 4.2 – Flue gas composition and properties.

	CO ₂	O ₂	N ₂	CO	F _{Hc}	m
Average	8.02	8.03	80.36	2.52	1.93	0.24
Median	7.93	8.30	80.17	2.44	1.60	0.24
Min	2.27	1.53	78.42	0.81	0.35	0.19
Max	13.73	15.87	84.64	4.44	6.15	0.36

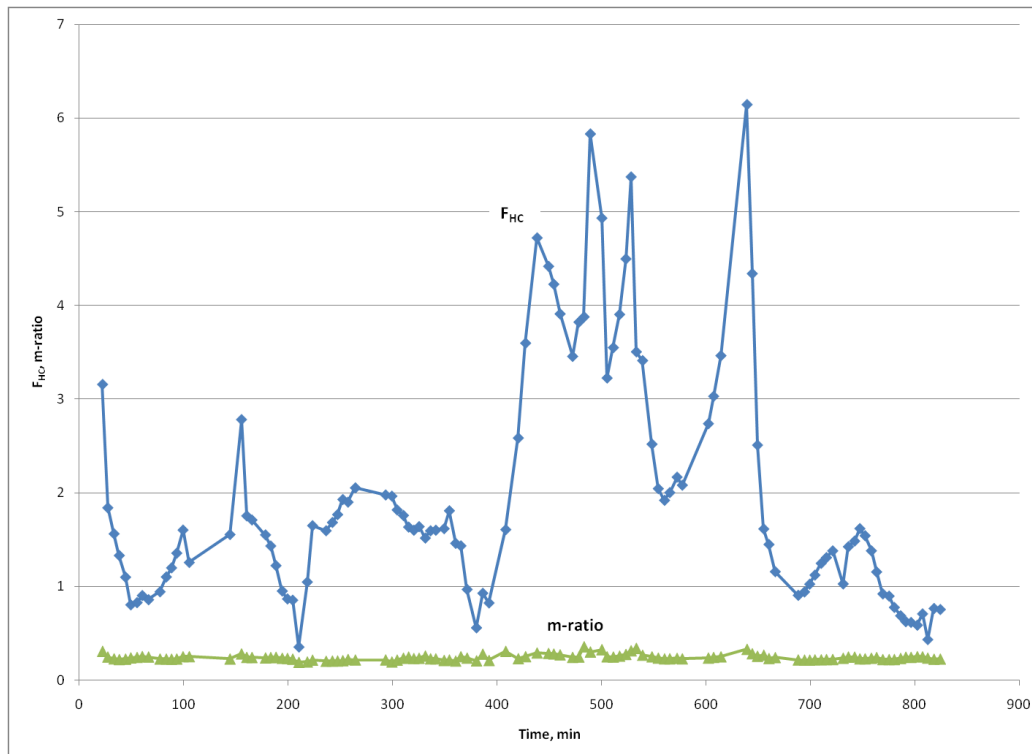


Fig. 4.3 Apparent H/C ratio and m-ratio for run no. 1 (base run).

Temperature profile of the combustion run is given in **Fig 4.4**. Temperatures of combustion front are not stable and vary from 506°C to 335°C. The reason for this temperature drop was described earlier. The average temperature of the combustion front is 430°C. The movement of the combustion front and its velocity is indicated in **Fig 4.5**. Velocity of combustion is not uniform, and changes with time. The average combustion front velocity is about 0.1 cm/min. This number is calculated from added trendline, and is quite low. In **Fig 4.6** I constructed temperature profile of combustion from data of fixed thermocouples. As you can see this graph confirms my assumption that there was a problem with combustion at certain time frame. An ideal case temperature should rise without plateaus or declines as we can see it on second and third points.

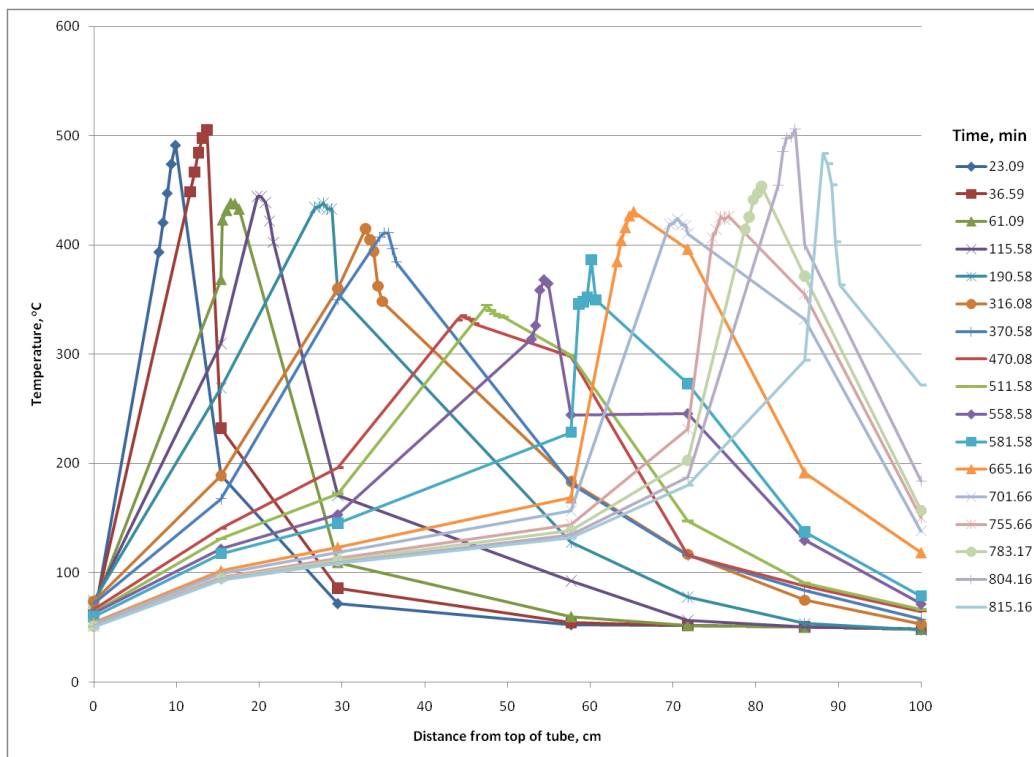


Fig. 4.4 – Temperature profiles for run no. 1 (base run).

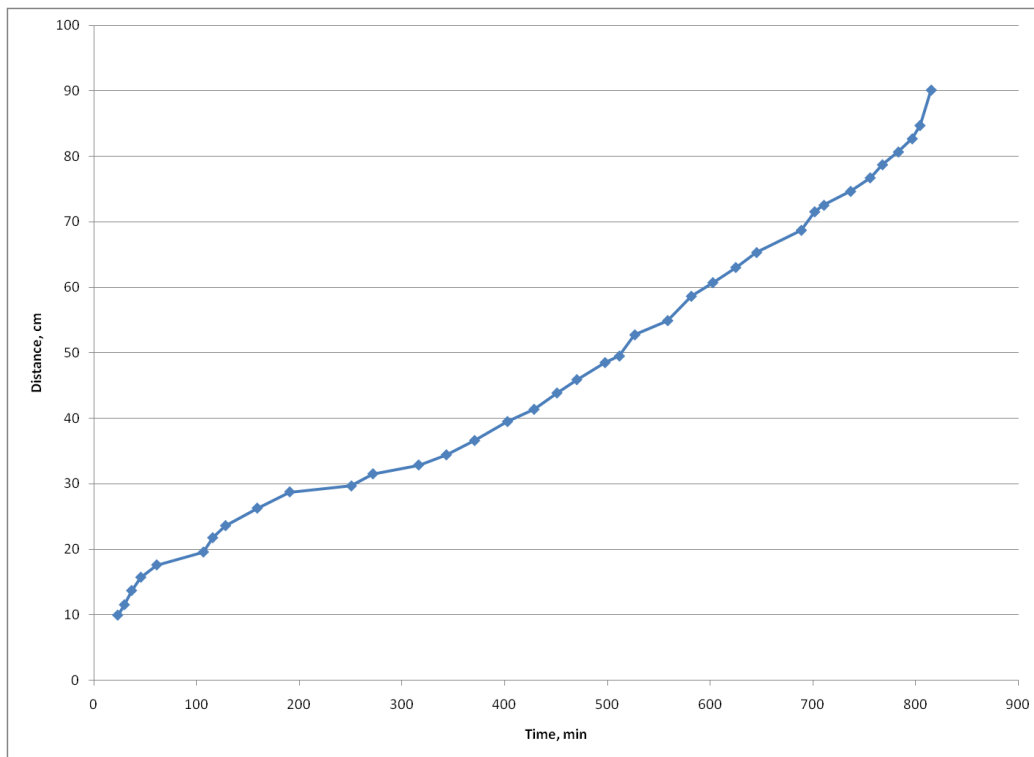


Fig. 4.5 – Combustion front velocity for run no. 1 (base run).

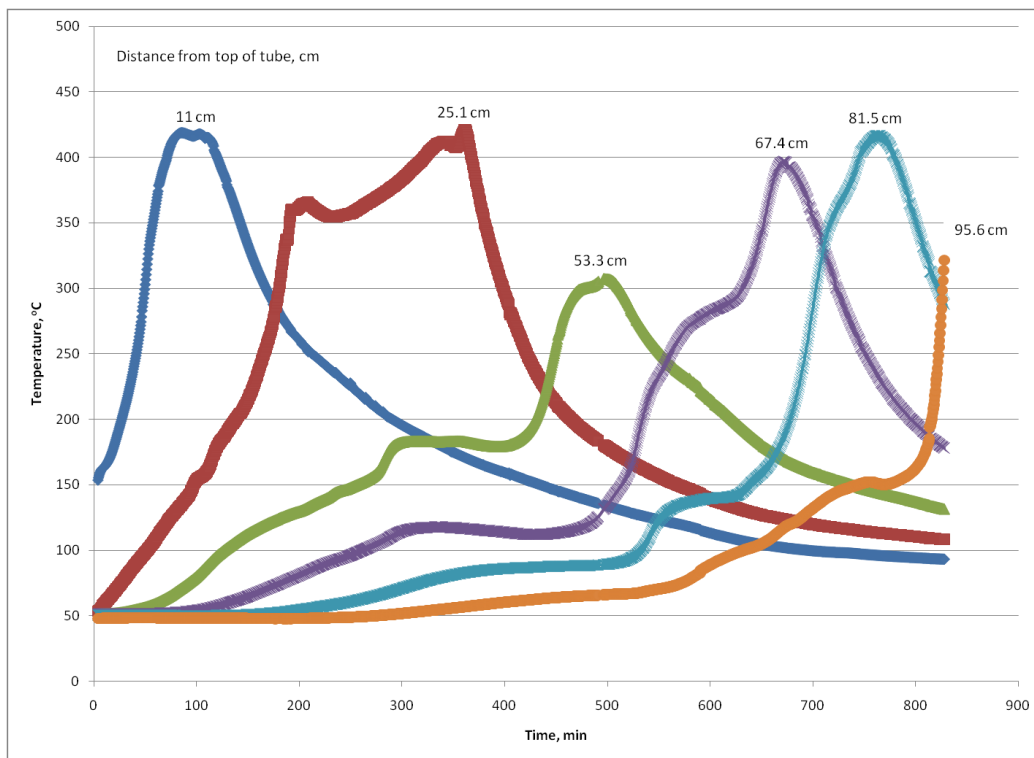


Fig. 4.6 – Temperature profile from fixed thermocouples for run no. 1 (base run).

Air injection rate, production and injection pressures versus time graph is built and presented in **Fig 4.7**. Air injection rate is almost constant through all the time of combustion and is about 3.1 L/min. Injection pressure increases up to 350 psi and drops slowly to normal ranges of about 300 psi. I think that it caused by oil bank that is created on the top layers of the tube. This oil bank got stuck in the layers before combustion front and limited air flow. This oil bank could also be the reason for the slow combustion front velocity. Difference of pressures comes to normal range at about 500 min, and exactly at the same time temperature of combustion front starts increasing (**Fig 4.4** and **Fig. 4.6**). Average injection and production temperatures are 316 psi and 296 psi respectively.

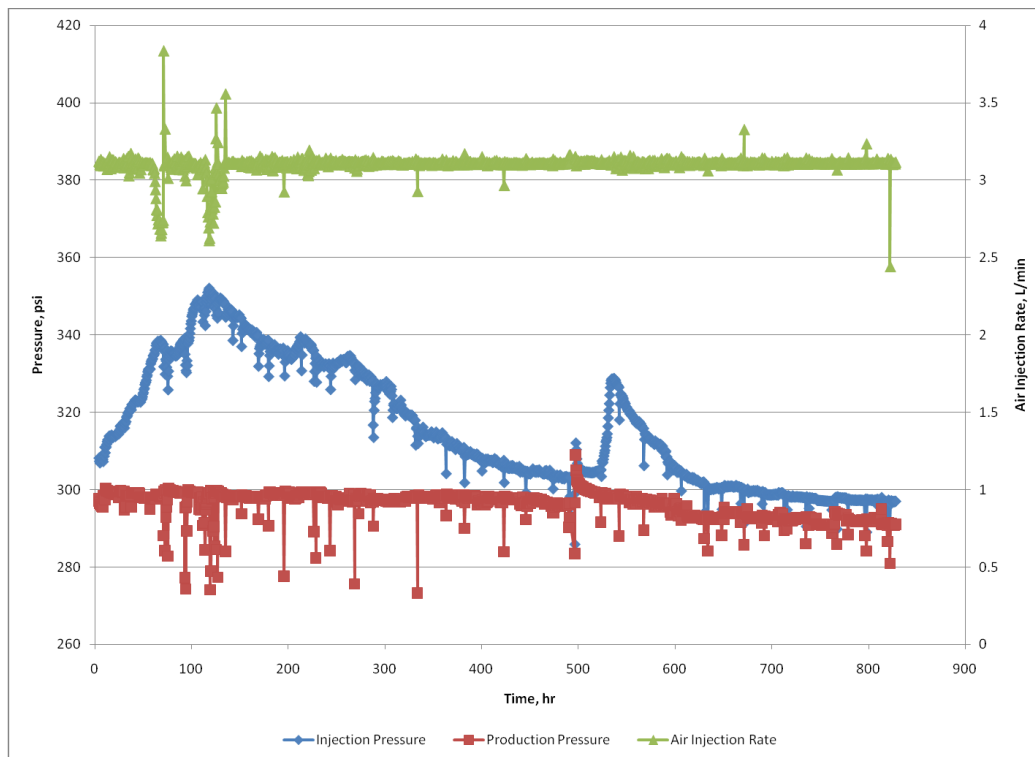


Fig. 4.7 – Injection and production pressures and air flow rate for run no. 1.

Water saturation for this run was only 12%. This amount of water is too low and part of it was withdrawn with flue gas. Remaining part of it created emulsion with oil and couldn't be separated. Therefore it was not possible to measure exact volume of produced oil and gas. Produced liquid weights were measured and presented as a graph in **Fig 4.8**. Cumulative volume of produced liquid is 972 g which is 81% of original fluid in place. Original fluid in place here is a volume of oil and water together inside the combustion tube. Cumulative volume of produced gas and its average rate versus time graph is shown in **Fig 4.9**. Average rate of produced gas is 2.7 L/min which is lower than the injection rate. This difference is created due to gas losses from separator while producing oil.

The densitometer was set at 50°C to enable the oil samples to be introduced into the instrument. Oil gravity was measured, while oil viscosity was measured at three different temperatures: 40°C, 50°C and 60°C. Produced oil gravity at the end of the run was 1.3°API higher than that in the original crude oil (**Fig 4.10**). The viscosity of the produced oil is calculated and constructed as a chart. As you can see from the graph viscosities are different for different temperatures. It also varies depending on time when oil samples were taken. There is a tendency that oil viscosities are higher in second point in comparison with other two points. In the last point we have the lowest viscosities as well as the highest oil gravity. The results indicate oil fractions distilled off at the combustion front, travel to and condense ahead.

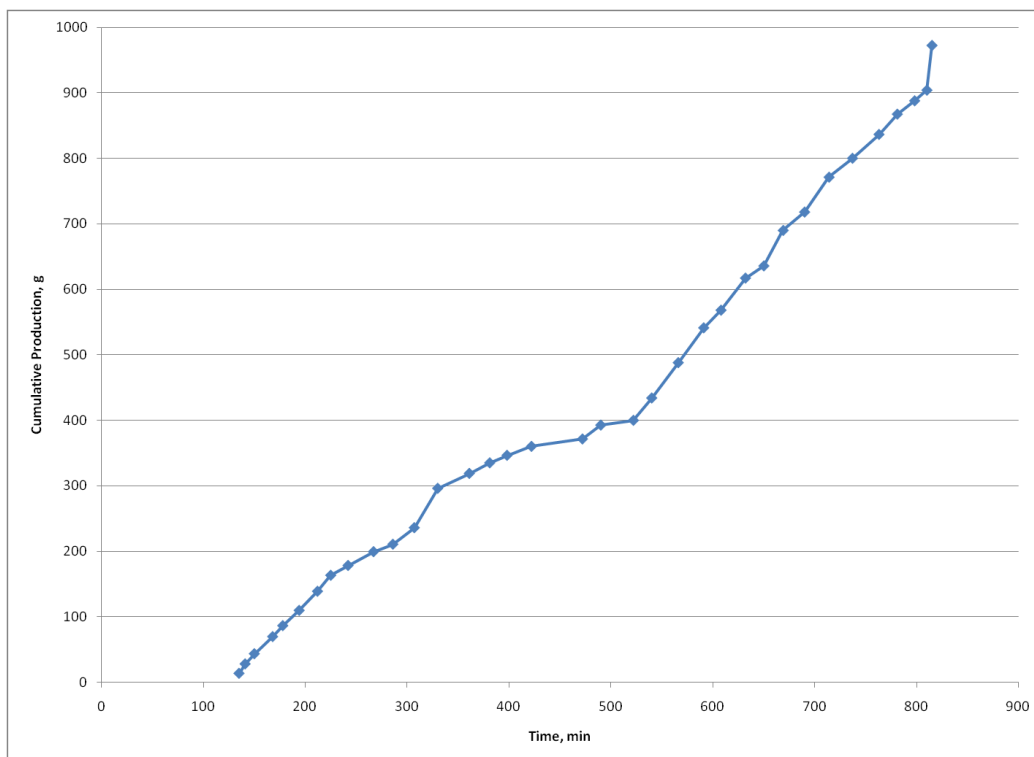


Fig. 4.8 – Cumulative fluid production for run no. 1 (base run).

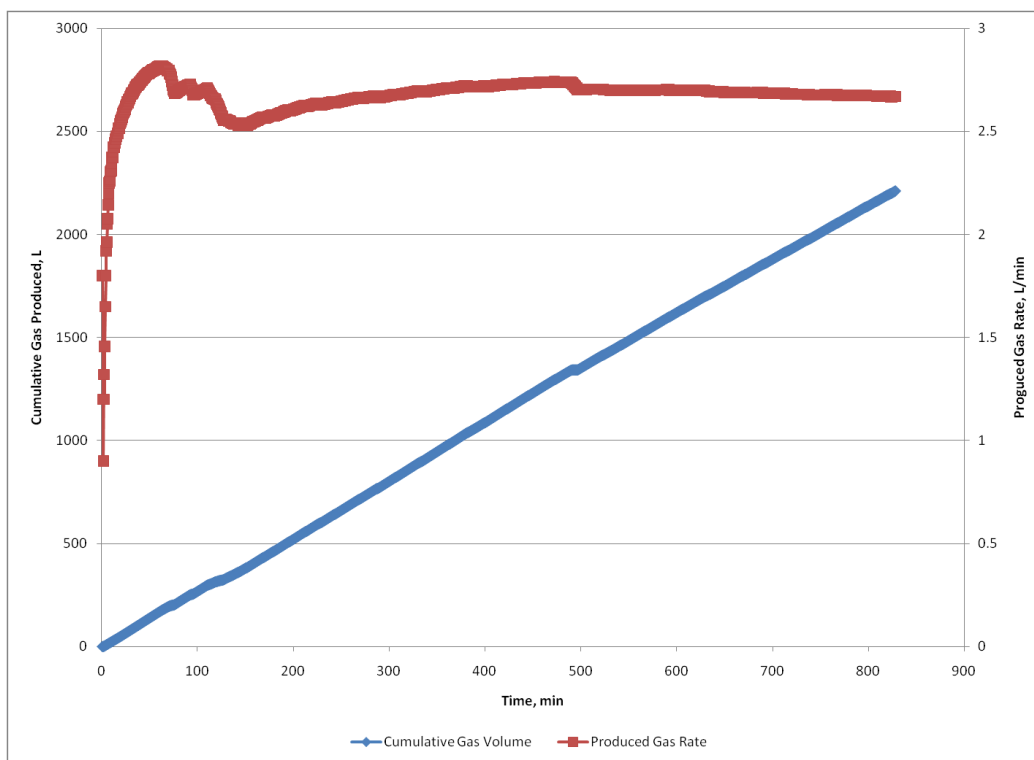


Fig. 4.9 – Cumulative produced gas volume and produced gas rates for run no. 1.

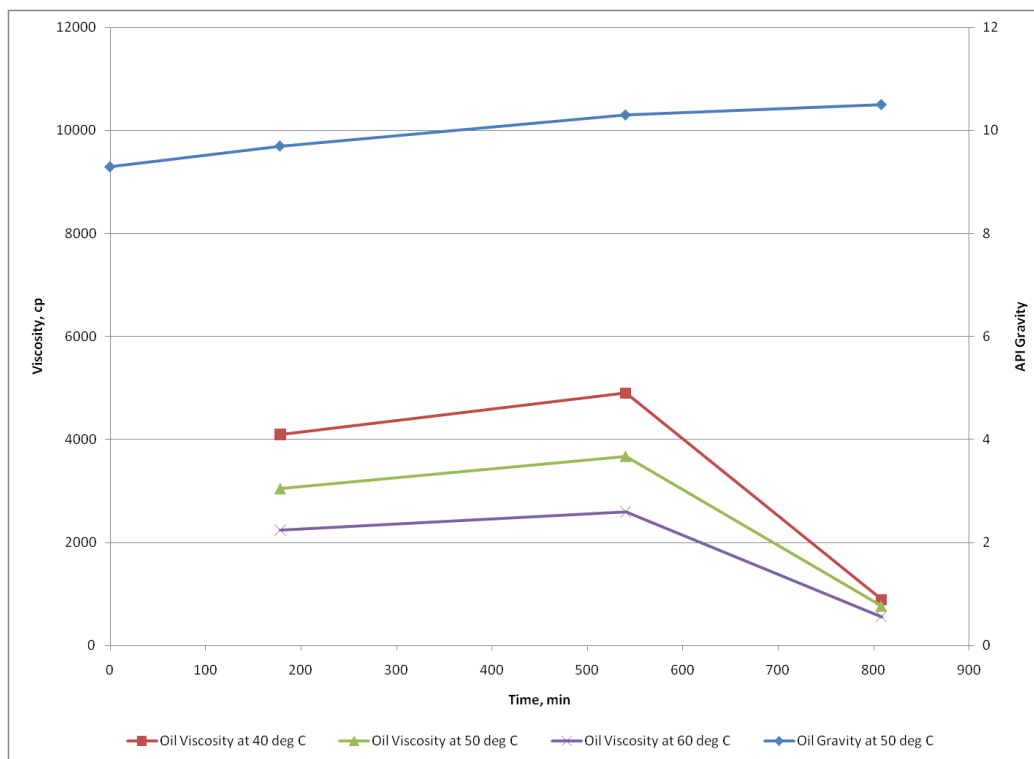


Fig. 4.10 – Produced oil gravity and viscosity for run no. 1 (base run).

4.3 Combustion run 2 - decalin and catalyst

Produced flue gas composition versus time graph is constructed and presented in **Fig 4.11**. As we can see from the chart, concentrations of oxygen and carbon dioxide fluctuate a lot. In one of the sections we produce more oxygen than carbon dioxide. The reason for this is probably due to air channeling which is created in the zone near to front and further. A portion of air is not used for combustion and bypasses the flame. The concentration of carbon monoxide decreases at the same time. Apparent H/C ratio and m-ratio versus time graph is shown in **Fig 4.12**. Apparent H/C ratio is more constant in comparison with base run which shows improvement of process. If we look at apparent H/C curve, we can see it increases rapidly at the same time (between 200 min and 300 min). The higher the apparent H/C ratio, the lower the oxidation temperature which leads to incomplete combustion. But overall image of combustion is fine, because apparent H/C is mostly less than 1. And average value of it is 1.14 which is way lower than base run without additives. From data of these two graphs we can clearly see that oxidation in this run is much more efficient compared to the first run. Average, median, minimum and maximum values of gas concentrations and apparent H/C and m-ratios are given in **Table 4.3**.

Table 4.3 - Flue gas composition and properties.

	CO₂	O₂	N₂	CO	F_{Hc}	m
Average	11.11	4.75	78.97	3.36	1.14	0.23
Median	12.11	3.51	78.95	3.66	1.00	0.23
Min	4.95	1.12	76.56	1.51	0.14	0.21
Max	15.47	12.27	82.32	4.40	3.25	0.28

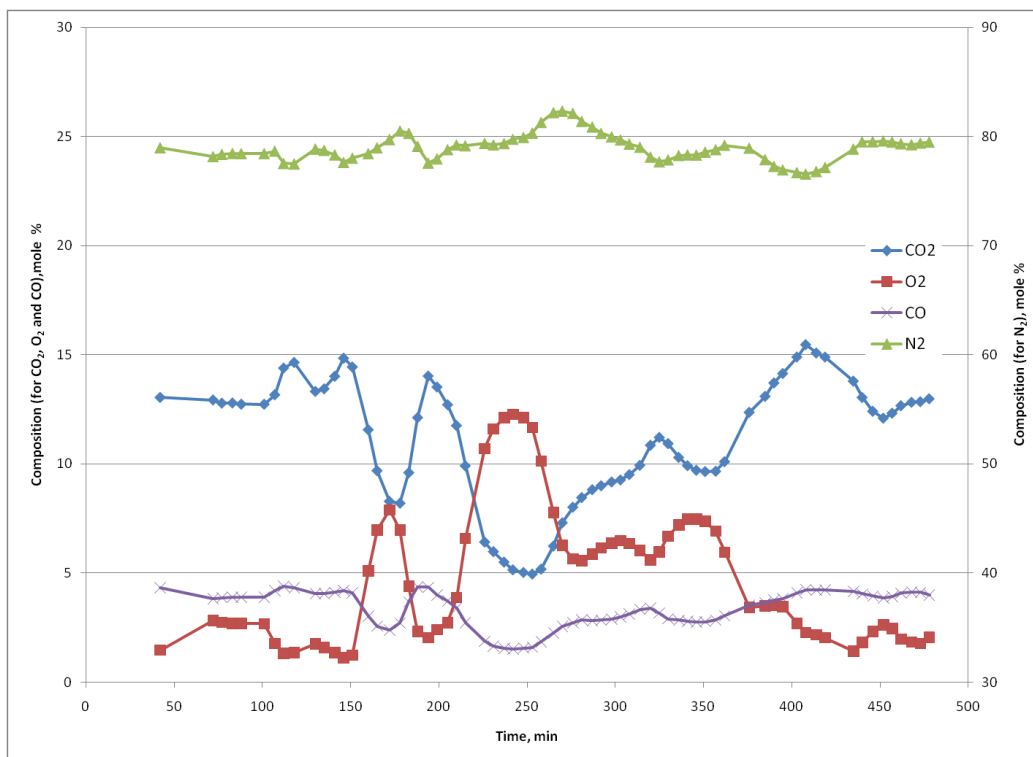


Fig. 4.11 – Produced gas composition for run no. 2.

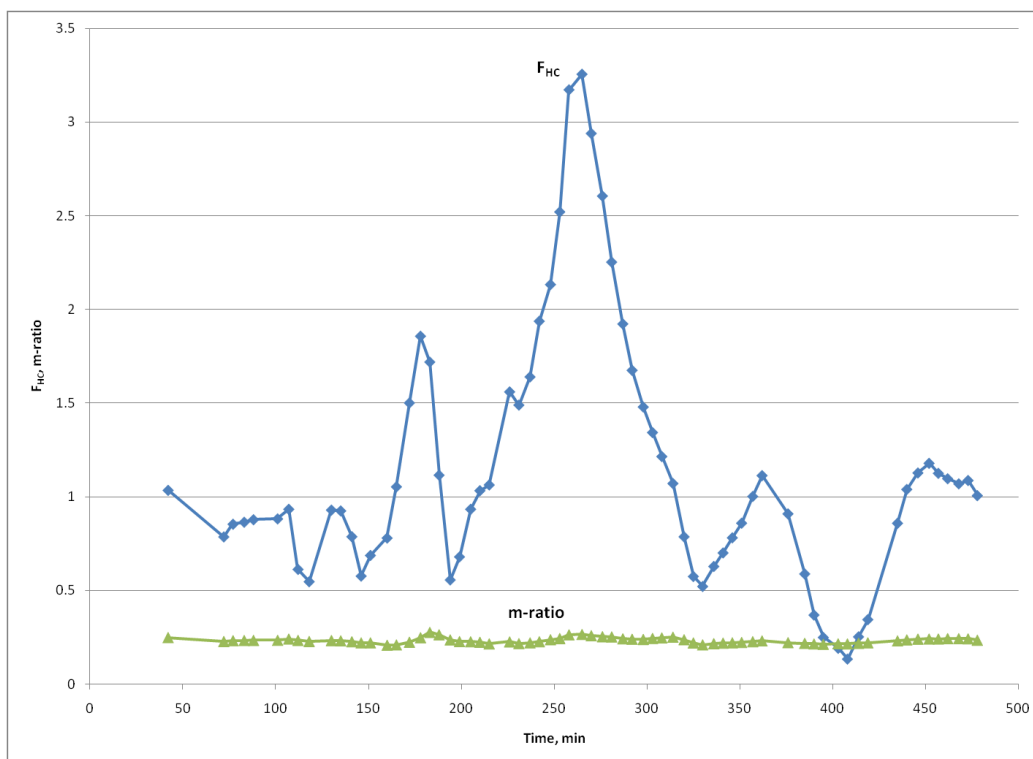


Fig. 4.12 Apparent H/C ratio and m-ratio for run no. 2.

Temperature profile of the combustion run is presented in **Fig 4.13**. Combustion front temperatures are quite uniform and mostly higher than 500°C. The average temperature of combustion front is 508°C. Improvement of temperature profile of combustion compared to first run is noticeable. One thing we really try to avoid in in-situ combustion is low temperature oxidation. LTO causes condensation reactions, which results in longer hydrocarbon chains and higher viscosity of oil. Catalyst brings to lower the activation energy which is required for combustion.

The movement of the combustion front and its velocity are shown in **Fig 4.14**. Velocity of the combustion is not uniform, and changes with time. Combustion front movement can be divided into three phases. In the first phase, the first 42 cm of the tube is considered where the average velocity of combustion front was 0.2 cm/min. Next phase is a segment between 52 cm and 56 cm where velocity of front is 0.04 cm/min. Combustion front recovers its initial velocity and next 34 cm goes at average velocity of 0.22 cm/min. I put the temperature profile of combustion from data of fixed thermocouples in **Fig 4.15**. From this graph we can see that at 300 min there is a plateau where temperature stopped increasing. It happened at the same time when combustion got stuck in the graph of combustion front velocity. There are two possible reasons for it. First, an oil bank was formed in this area which did not move further. It took time to burn all this deposition. Second possible reason is that most part of the oil moved through a channel to the bottom flange without assisting combustion.

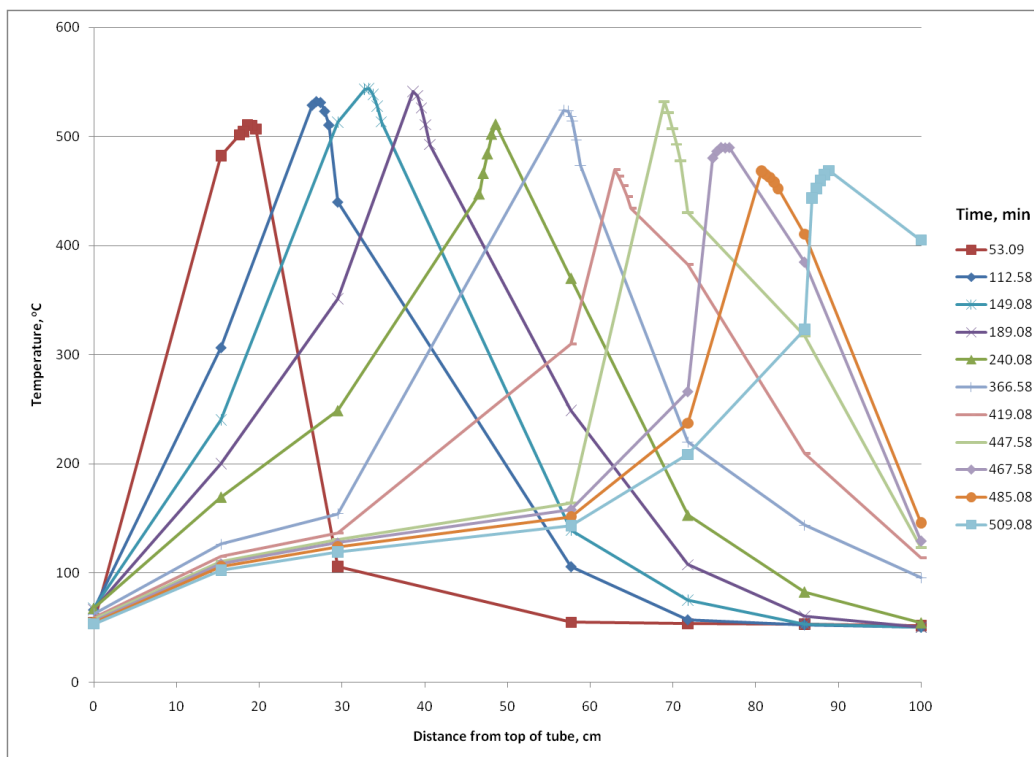


Fig. 4.13 – Temperature profiles for run no. 2.

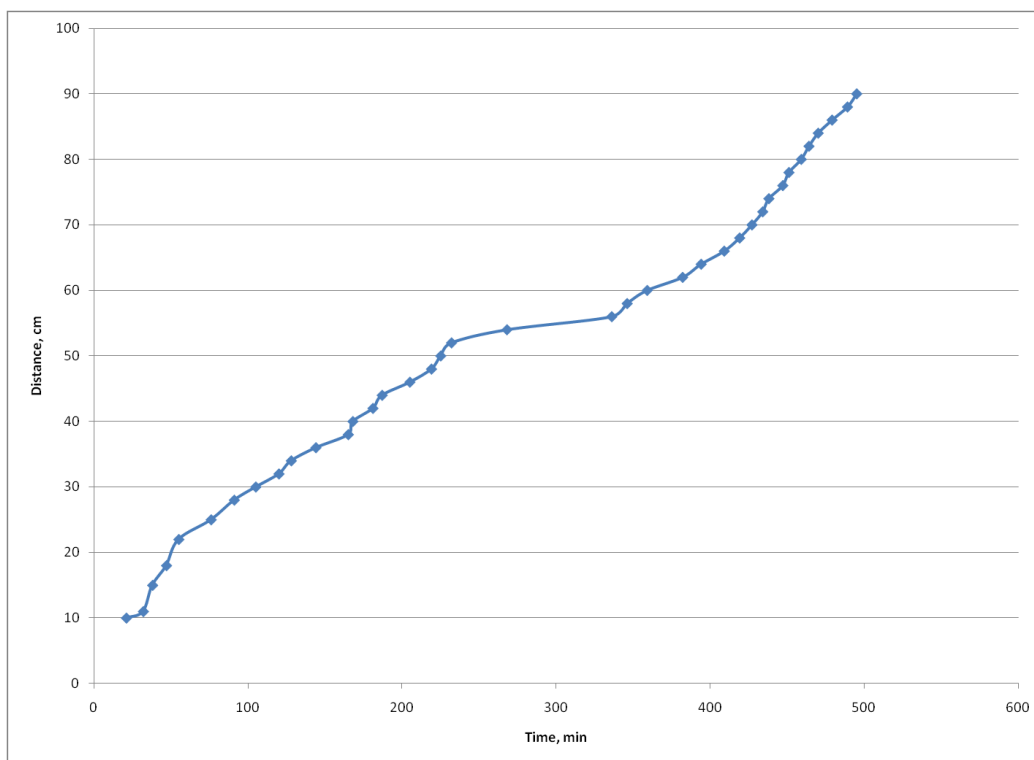


Fig. 4.14 – Combustion front velocity for run no. 2.

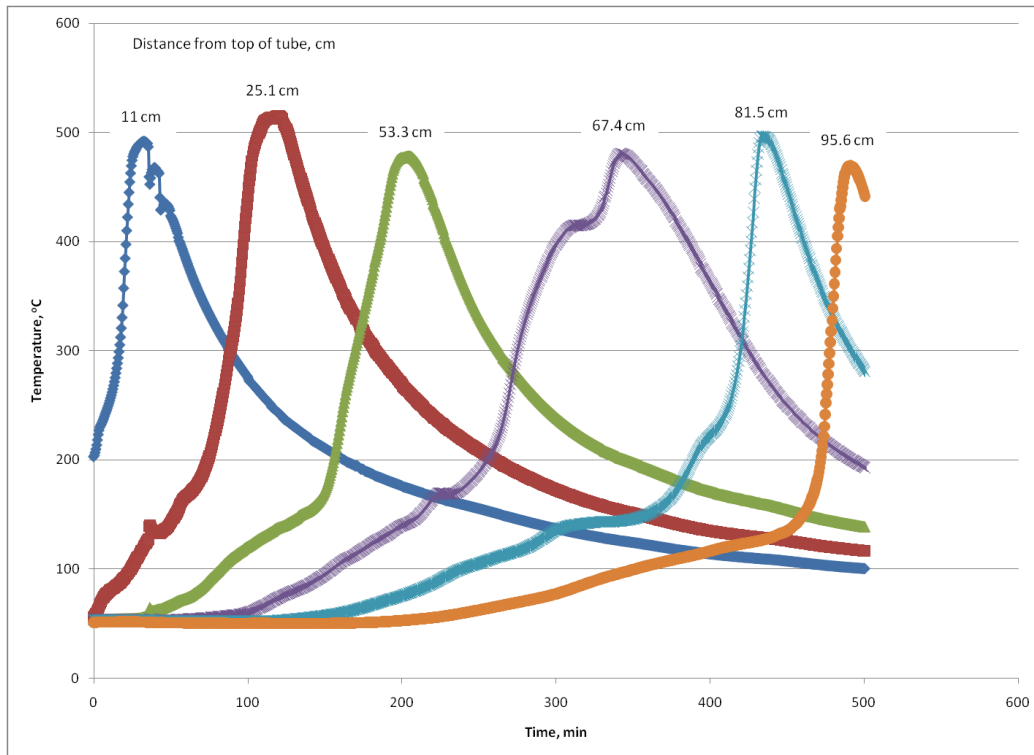


Fig. 4.15 – Temperature profile from fixed thermocouples for run no. 2.

Air injection rate, production and injection pressure versus time graph are presented in **Fig 4.16**. Air injection rate is almost constant through all the time of combustion and is about 3.1 L/min. Injection pressure increases up to 350 psi and drops slowly to about 300 psi. I think that it is caused by oil bank that is created on the top layers of tube. This oil bank got stuck in the layers before combustion front and limited air flow. Average injection and production temperatures are 317 psi and 300 psi respectively.

Water saturation for this run was only 12%. This amount of water is too low and part of it was produced with the flue gas. Remaining part of it created emulsion with oil and couldn't be separated. Therefore it was not possible to measure the exact volume of produced oil and gas. Produced liquid weights were measured and presented as a graph in **Fig 4.17**. Production of liquid started about at the same time as in original case at 130

min. Cumulative volume of produced liquid is 1005 g which is 88% of original fluid in place. Cumulative volume of produced gas and its average rate versus time graph is shown in **Fig 4.18**. Average rate of produced gas is 2.7 L/min, which is lower than injection rate. This difference is created due to gas losses from separator while producing oil.

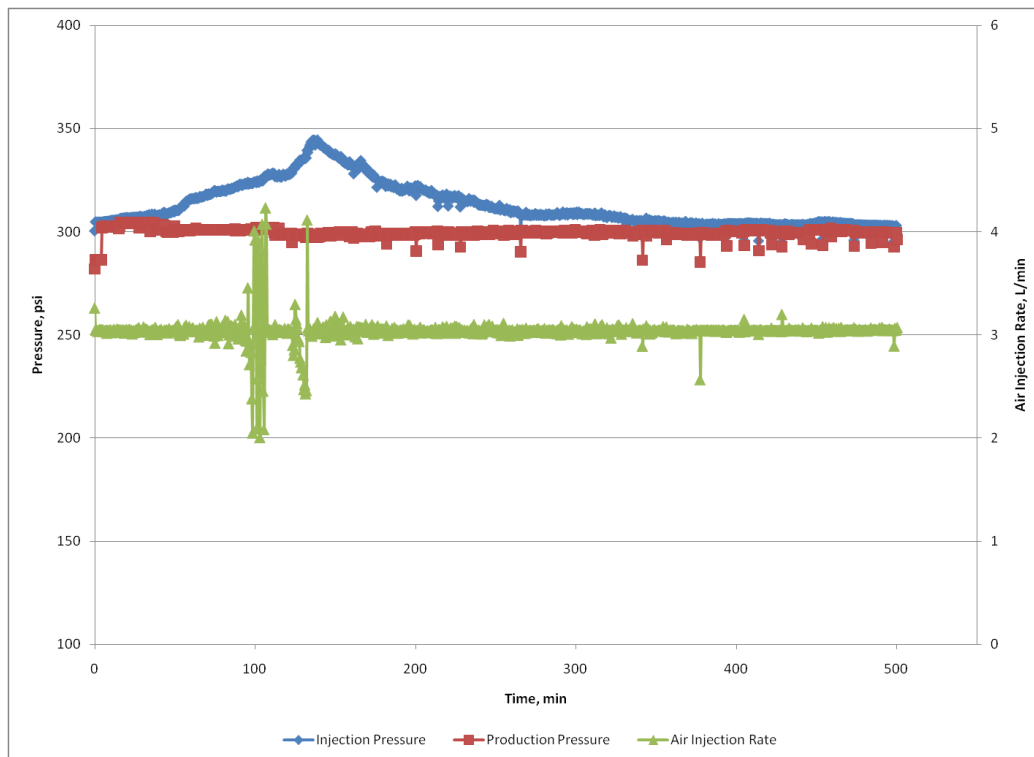


Fig. 4.16 – Injection and production pressures and air flow rate for run no. 2.

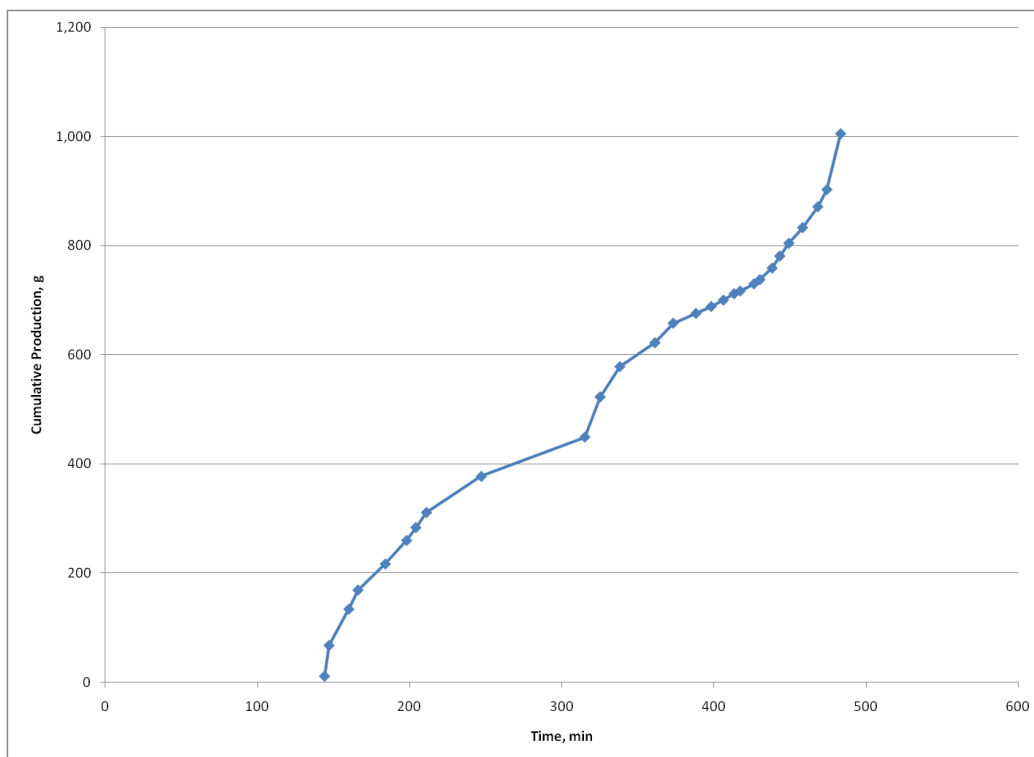


Fig. 4.17 – Cumulative fluid production for run no. 2.

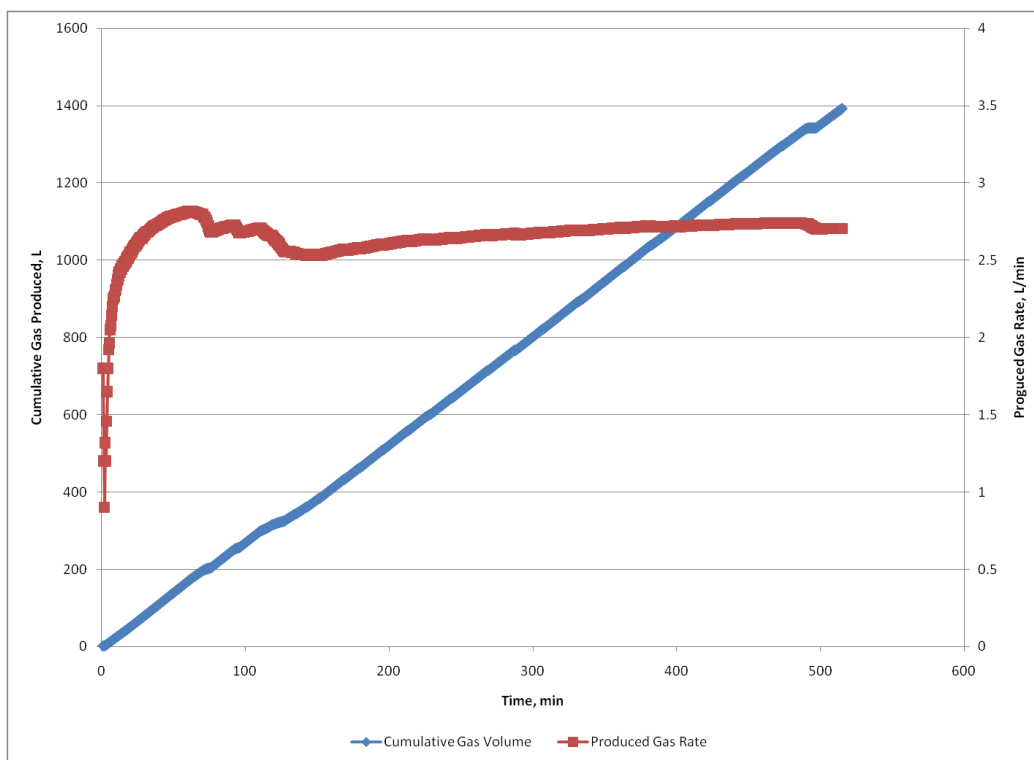


Fig. 4.18 – Cumulative produced gas volume and produced gas rates for run no. 2.

The densitometer was set at 50°C to enable the oil samples to be introduced into the instrument. Oil gravity was measured, while oil viscosity was measured at three different temperatures: 40°C, 50°C and 60°C. Produced oil gravity at the end of run was 3.2 °API higher than at the original crude (**Fig 4.19**). The viscosity of the produced oil decreased compared to the base run. The graph of viscosities also changed its shape, and viscosity of second point is lower than first one now. Decrease of viscosity and increase of gravity occurs due to upgrading of oil during combustion. Light hydrocarbon content increase because of cracking and hydrogen supplied by decalin.

This run took only 480 min, which is great improvement in comparison with previous run. It is almost two times faster, and gives better results in recovery of hydrocarbons and in upgrading of oil.

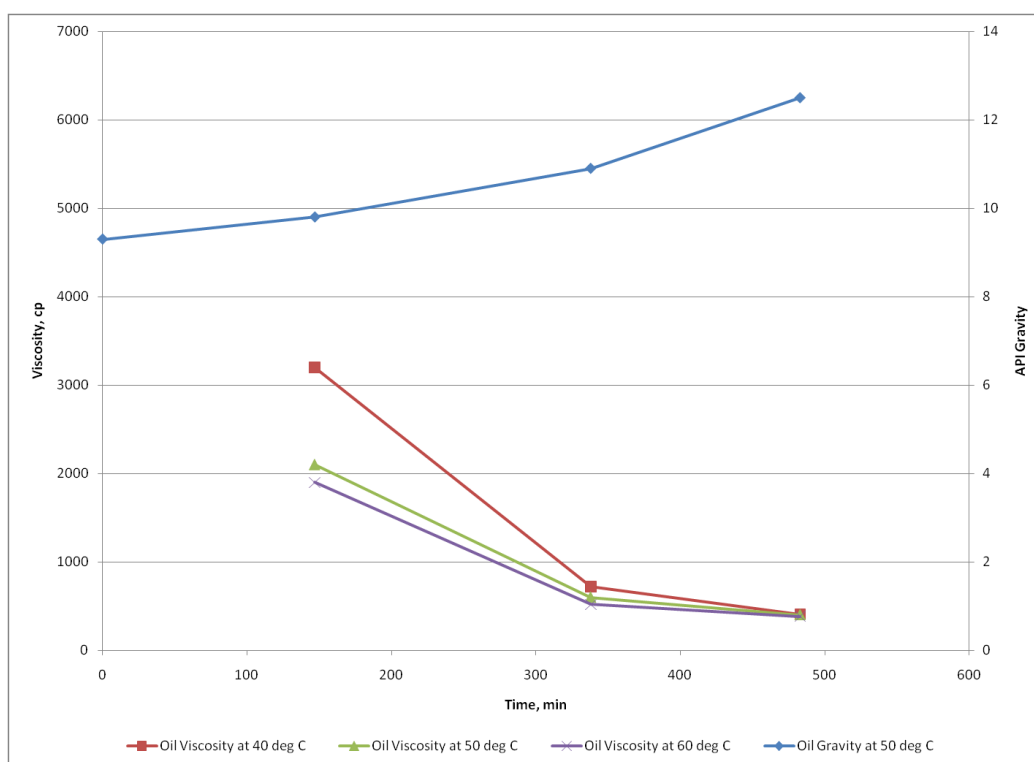


Fig. 4.19 – Produced oil gravity and viscosity for run no. 2.

4.4 Combustion run 3 - decalin and catalyst

Stable composition of produced flue gases is observed during the run as shown in **Fig 4.20**. Average concentration of oxygen is 2.3%. **Fig 4.21** I presents apparent H/C ratio and m-ratio versus time graph. Apparent H/C ratio is more constant in comparison with two previous runs which show improvement in combustion. Apparent H/C ratio is much lower even in comparison with the second experiment. This result indicates the absence of low temperature oxidation and the predominance of distillation as the fuel deposition mechanism. The average value of the ratio is 0.69 and maximum value is 1.55. And average value of it is 1.14 which is lower than the base run without additives. The m-ratio is constant and has an average value of 0.22. From data of these two graphs we can clearly see that oxidation in this run is much more efficient compared to the first two runs. Average, median, minimum and maximum values of gas concentrations and apparent H/C and m-ratios are given in **Table 4.4**.

Table 4.4 - Flue gas composition and properties.

	CO₂	O₂	N₂	CO	F_{HC}	m
Average	14.20	2.27	79.79	3.91	0.69	0.22
Median	14.46	1.69	79.93	4.06	0.69	0.22
Min	9.84	0.81	77.09	2.61	0.04	0.18
Max	17.42	6.95	82.11	4.74	1.55	0.25

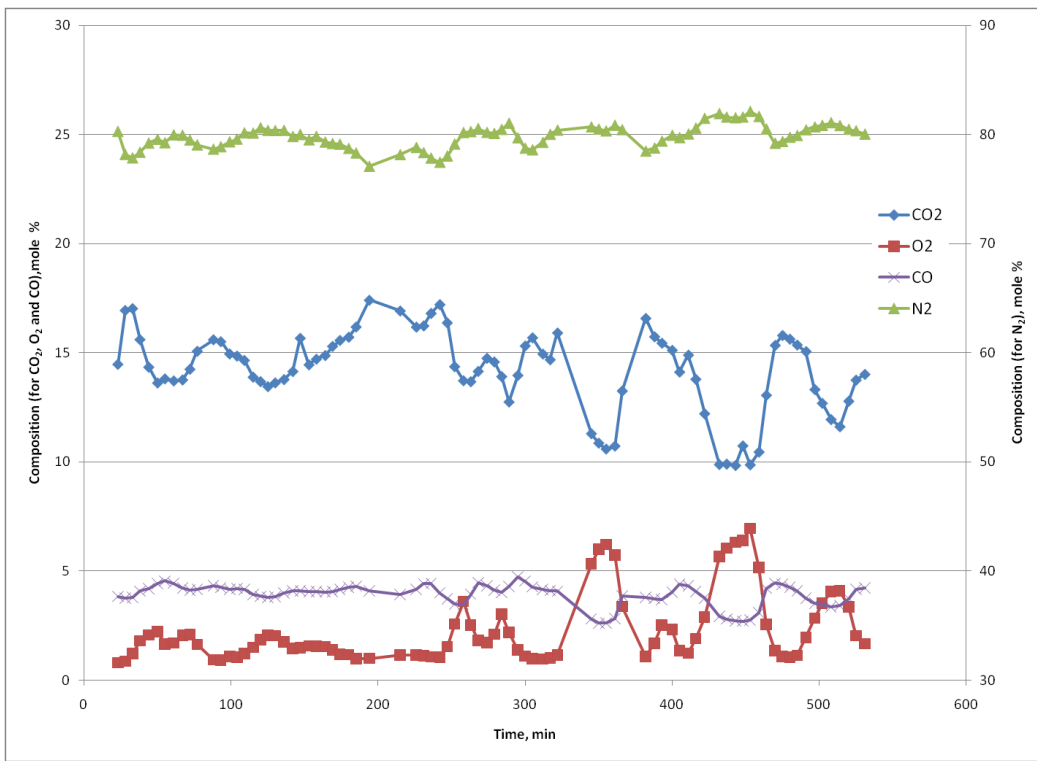


Fig. 4.20 – Produced gas composition for run no. 3.

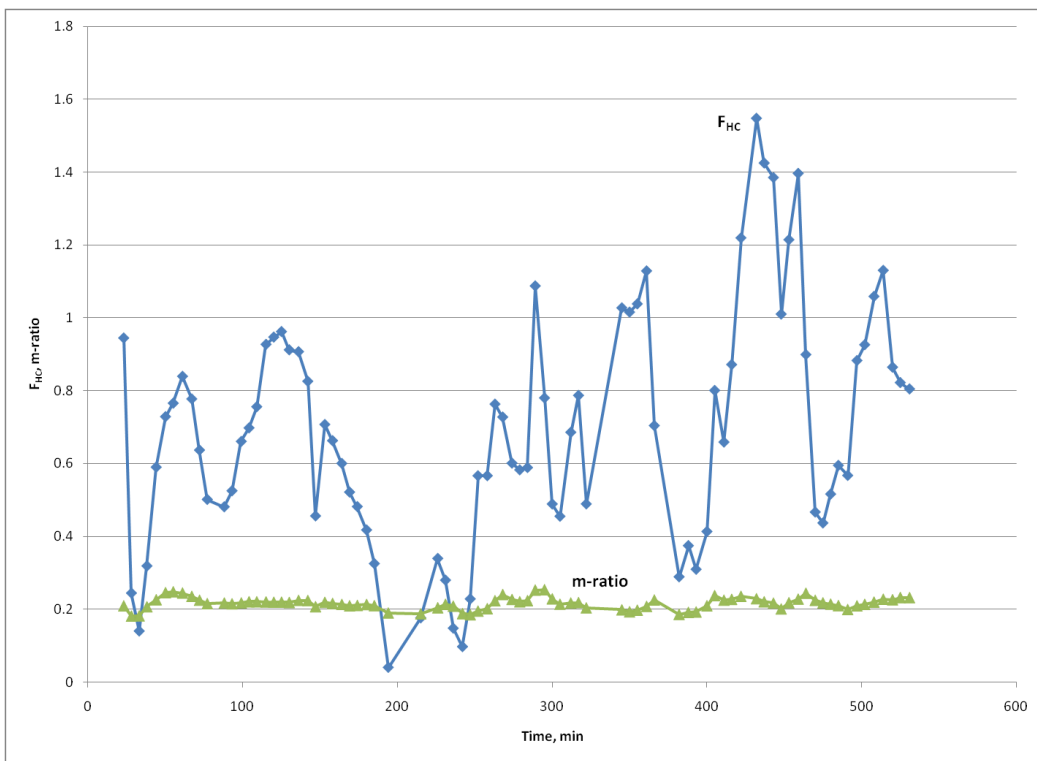


Fig. 4.21 Apparent H/C ratio and m-ratio for run no. 3.

From the temperature profile (**Fig 4.22**) we notice that temperatures of this combustion are markedly higher than in the previous two runs. Combustion front temperatures go as high as 635°C and the average temperature of combustion front is 563°C which excludes the existence of LTO. One thing we really try to avoid in in-situ combustion is low temperature oxidation. LTO causes condensation reactions, which results in longer hydrocarbon chains and higher viscosity of oil. Catalyst brings to lower activation energy required for combustion.

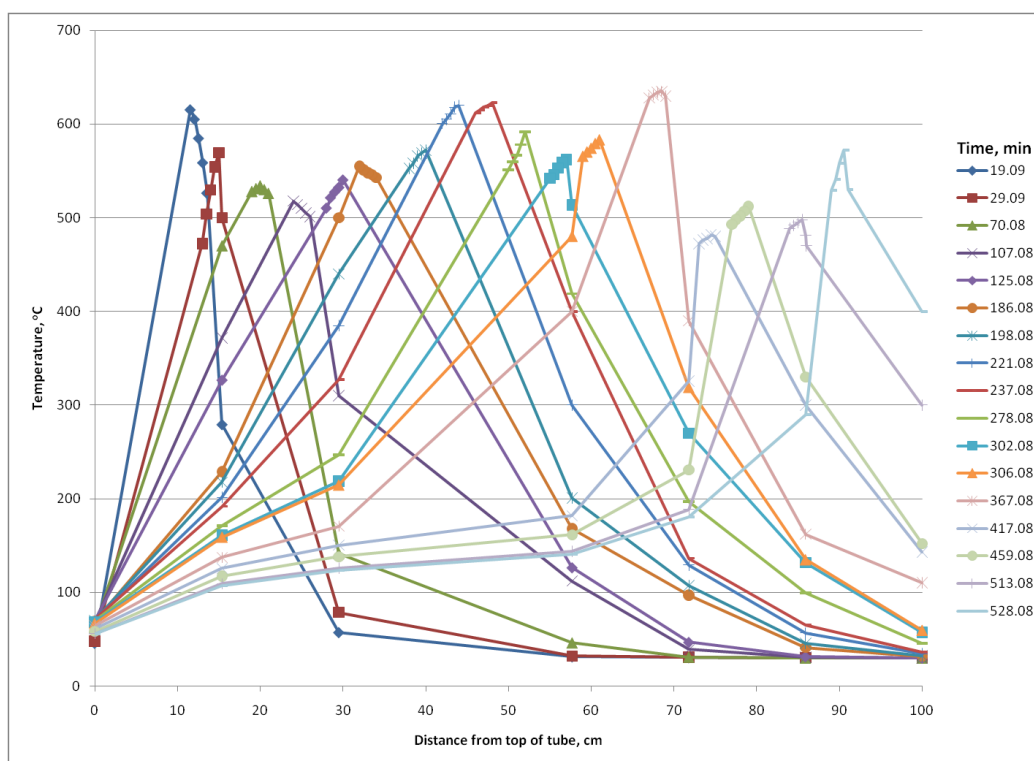


Fig. 4.22 – Temperature profiles for run no. 3.

Combustion front velocity and its movement are indicated in **Fig 4.23**. The movement of combustion is stable and has a uniform velocity unlike the previous two experiments. The combustion front velocity is 0.16 cm/min. The temperature profile of combustion

from data of fixed thermocouples is presented in **Fig 4.24**. Improved performance of combustion is clearly observed. There are no plateaus or declines as observed in the base run, which confirms the beneficial effects of decalin and catalyst.

The production and injection pressures and air injection rate versus time graph are plotted in **Fig 4.25**. Air injection rate is almost constant through all the time of combustion and is about 3.1 L/min. Injection pressure increases up to 324 psi and drops slowly to about 300 psi. The injection pressure increase is probably caused by the oil bank that is created in the middle of the tube. Average injection and production temperatures are 305 psi and 297 psi respectively.

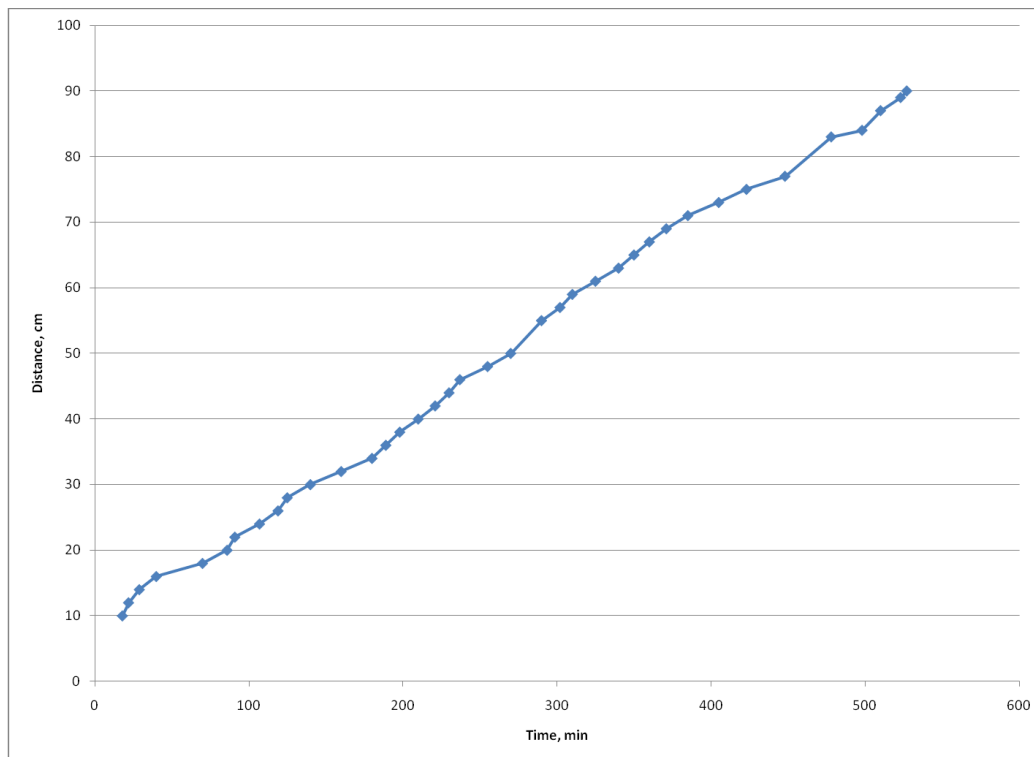


Fig. 4.23 – Combustion front velocity for run no. 3.

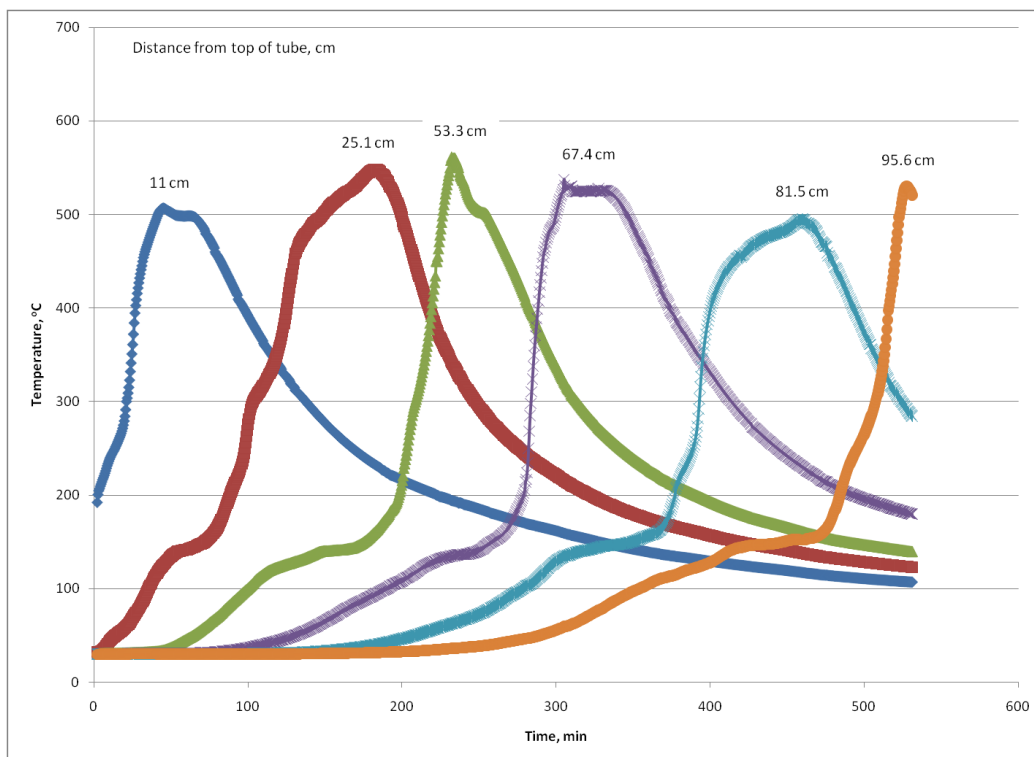


Fig. 4.24 – Temperature profile from fixed thermocouples for run no. 3.

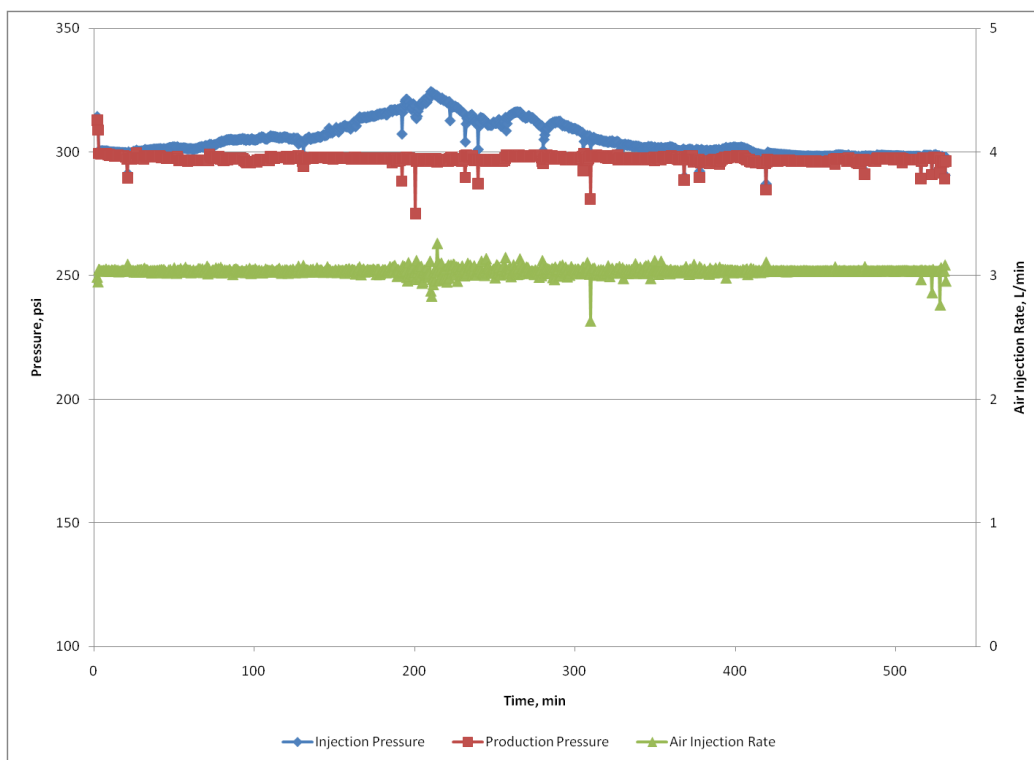


Fig. 4.25 – Injection and production pressures and air flow rate for run no. 3.

Water saturation for this run was only 12%. This amount of water is quite low and part of it was produced with the flue gas. Remaining part of it created emulsion with oil and couldn't be separated. Therefore produced liquid weights were measured and presented as a graph in **Fig 4.26**. Production started at 180 min which is late in comparison with the previous two runs. If we do not consider the base run, we can see analogy in the two last runs. In both of them production started when combustion front was at 35 cm from the top flange. Due to differences in velocities production times were different. Cumulative volume of produced liquid is 1002 g which is 88% of original fluid in place. Cumulative volume of produced gas and its average rate versus time graph is shown in **Fig 4.27**. Average rate of produced gas is 2.7 L/min which is lower than injection rate. This difference is created due to gas losses from separator while producing oil.

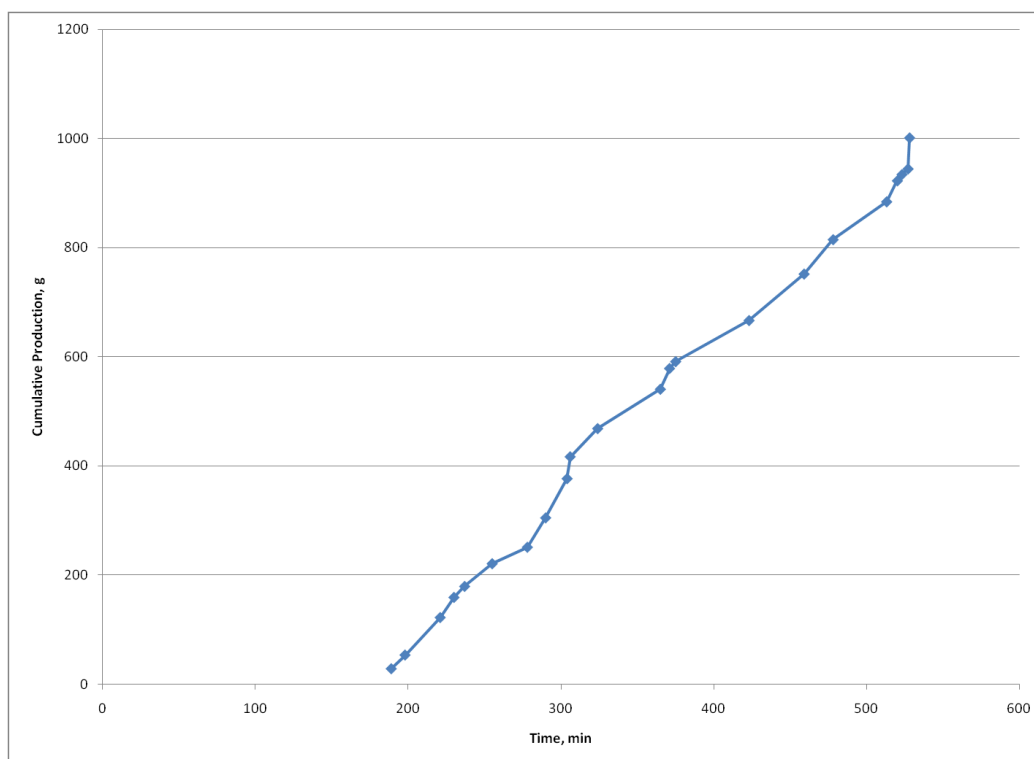


Fig. 4.26 – Cumulative fluid production for run no. 3.

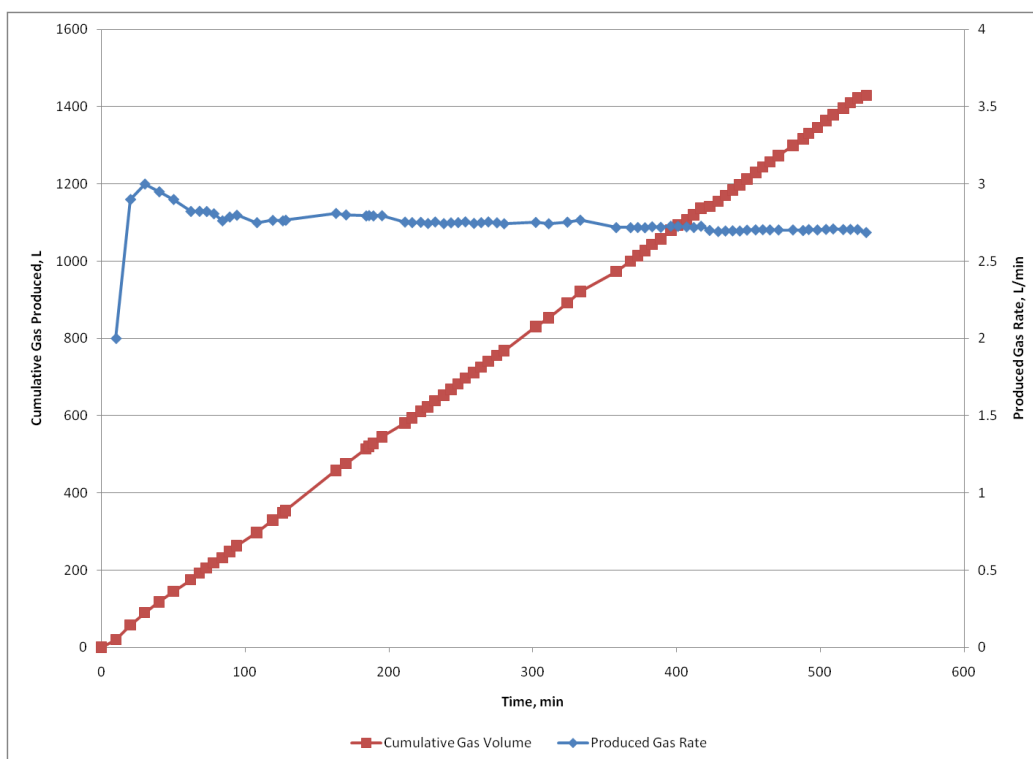


Fig. 4.27 – Cumulative produced gas volume and produced gas rates for run no. 3.

Oil gravity was measured at 50°C while viscosity was measured at three different temperatures: 40°C, 50°C and 60°C. Produced oil gravity at the end of the run was 5 °API higher than that of the original crude (**Fig. 4.28**). This is the best upgrading performance among all combustion runs. The viscosity of the produced oil decreased in comparison with base run with original crude oil. Decrease of viscosity and increase of gravity occurs due to upgrading of oil during combustion. Light hydrocarbon content increase because of cracking and hydrogen supplied by decalin.

This run took only 520 min, which is great improvement in comparison with the base run but is slower than second run. Cumulative produced fluid was almost the same as in second run and almost repeated the experiment.

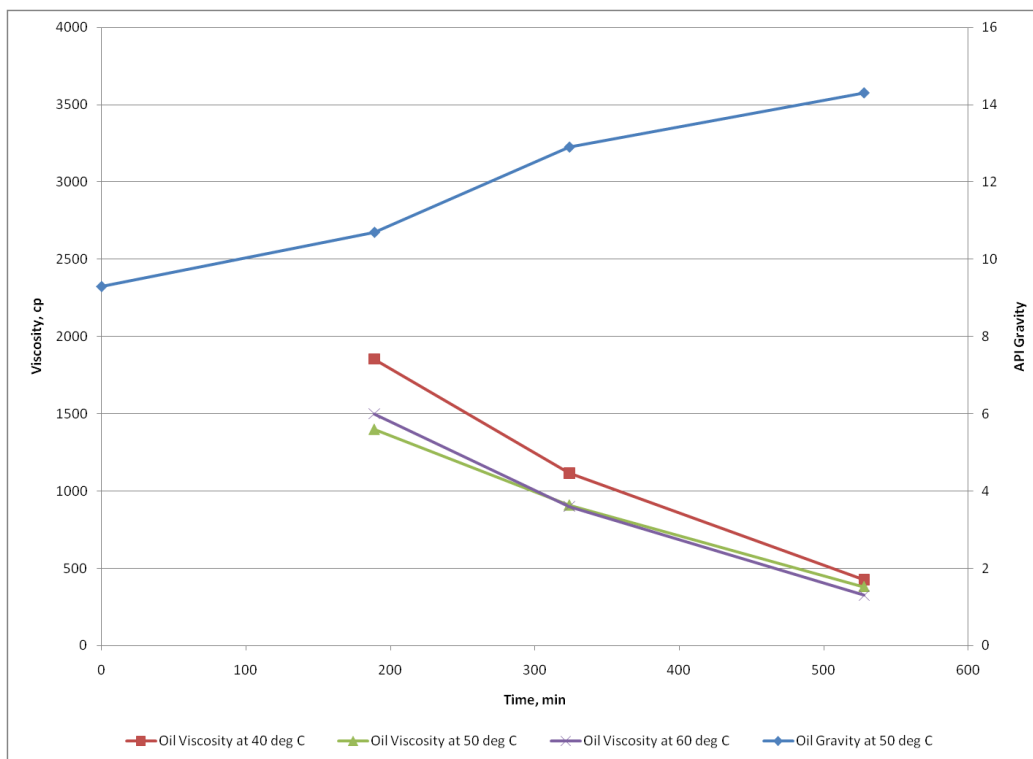


Fig. 4.28 – Produced oil gravity and viscosity for run no. 3.

4.5 Comparison and discussion of results

In this section I compare the three runs to evaluate upgrading and recovery enhancing abilities of decalin and organometallic catalyst mixture. In addition, the performances of decalin and tetralin as a hydrogen donor are compared. Data of combustion experiment with tetralin as a hydrogen donor is taken from the M.S. thesis of Palmer. (Palmer-Ikuku, 2009)

The most important parameter to evaluate the performance of decalin and a catalyst mixture is the oil recovery factor. **Fig 4.29** shows a graph of oil recovery factors versus time for the three runs. Second and third run showed higher oil recovery and much lower time of combustion. Liquid recovery from the base run is 81% while adding decalin and catalyst increased recovery by 7%. To compare effectiveness of decalin and tetralin I constructed oil recovery factors graph (**Fig 4.30**). As we can see, production from decalin happens more rapidly and finishes earlier. I think that it is due to differences of original oil in place. Weight of oil in tube in tetralin experiment is 500 g, while in the decalin experiment the weight of oil is about 1 kg. So in tetralin experiment less amount of oil is required to be produced. The graph with produced liquid weight versus time is presented in **Fig 4.31**. This chart defines the situation better and shows that production enhancing abilities of decalin surpasses. Supremacy is reflected in less time to produce the same amount of oil and 2% higher recovery by the end of combustion.

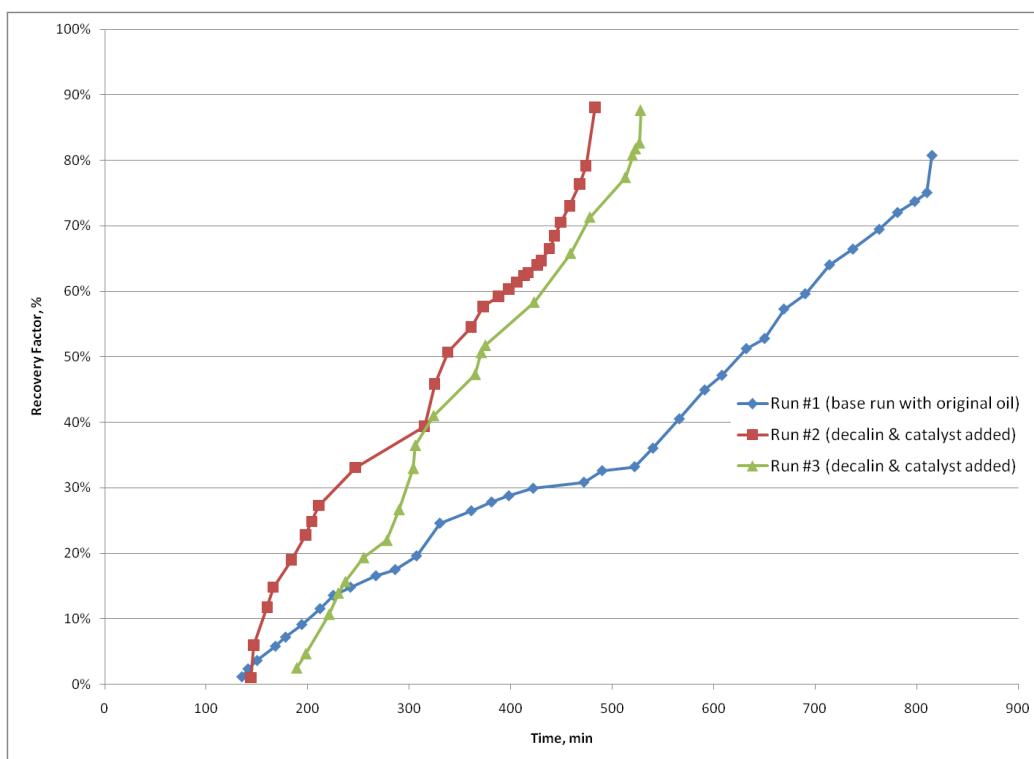


Fig. 4.29 – Recovery factors for all runs.

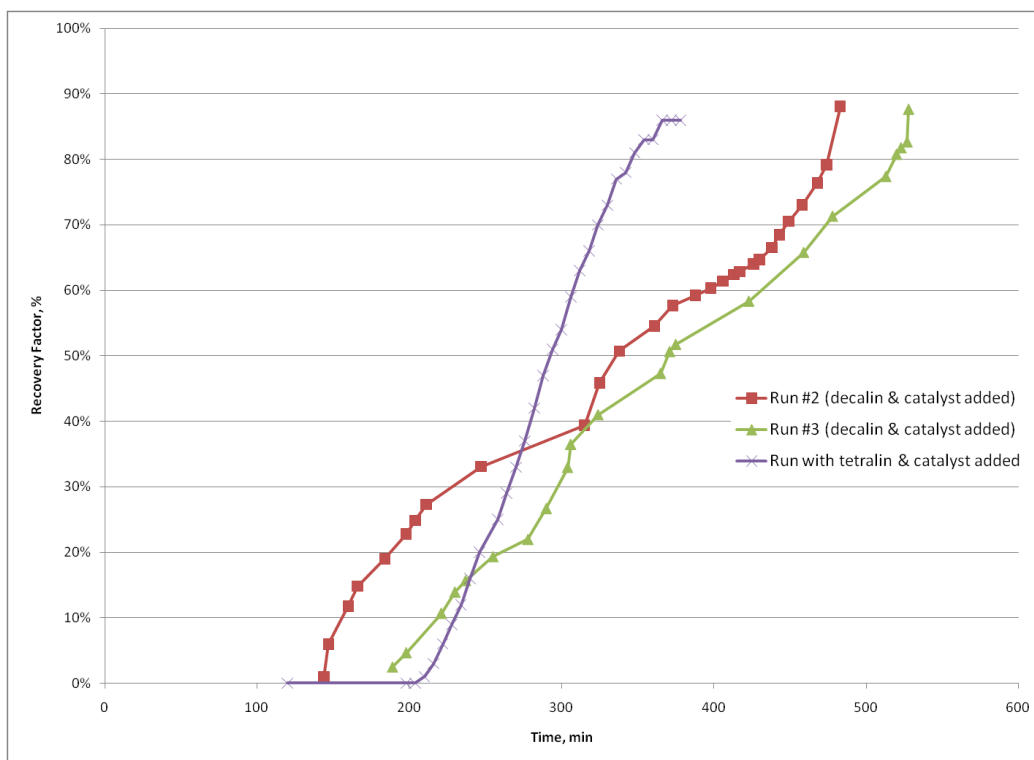


Fig. 4.30 – Recovery factors for runs with decalin and tetralin.

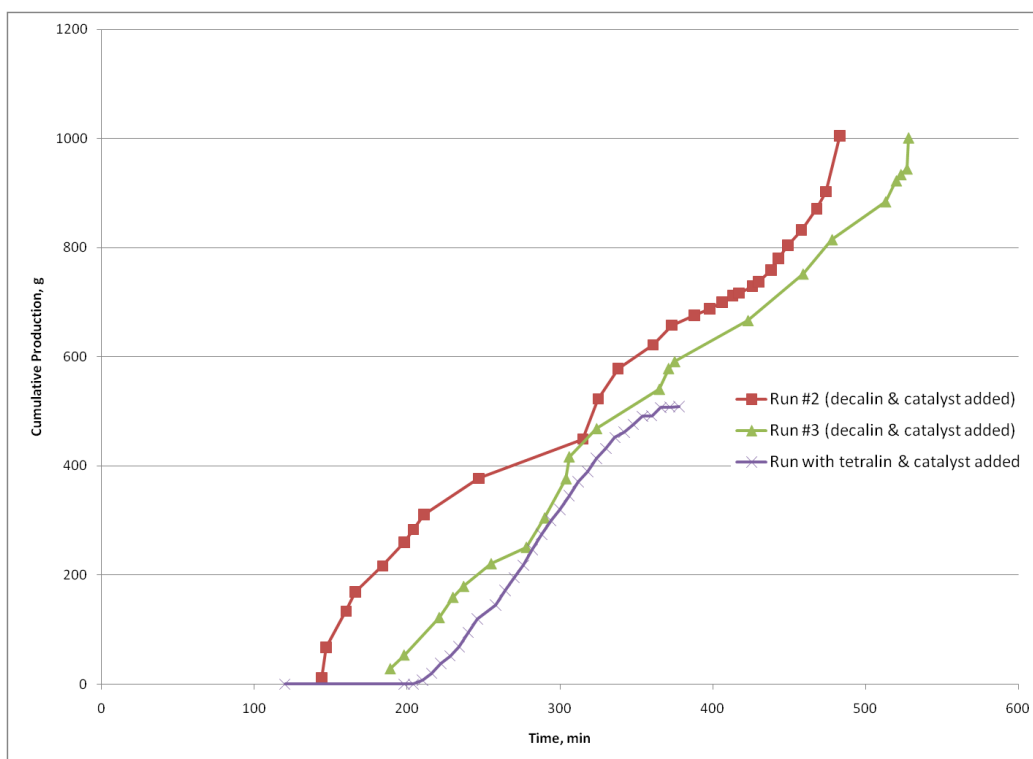


Fig. 4.31 – Cumulative oil production for runs with decalin and tetralin.

To evaluate upgrading abilities of additives we compared their API gravities and viscosities. From the graph of oil gravities versus time presented in **Fig 4.32** it is obvious that additives assist in produced oil upgrading. The API gravity of oil at the end of the experiment increased for 2 and 4 degrees API in experiments 2 and 3, respectively, in comparison with the base run. The oil gravity from run with tetralin (Palmer-Ikuku, 2009) also shows about 2 degrees API higher than the base run, except for the last data which was about 6 degrees API higher.

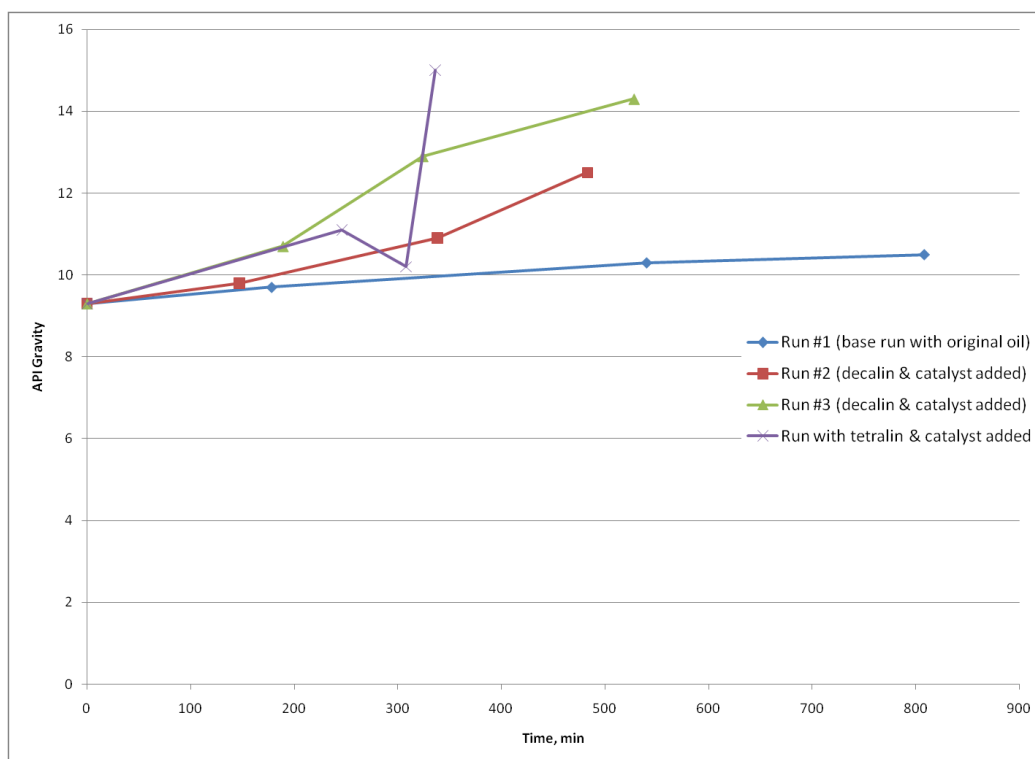


Fig. 4.32 – Produced oil gravity for all runs.

One indirect parameter by which we can judge on upgrading happening during combustion is apparent H/C ratio. The large apparent atomic hydrogen-carbon ratio is a result of oxygen being consumed in LTO reactions, which do not produce carbon-oxides. The viscosity and boiling range of the crude oil is increased because of LTO (Mamora and Brigham, 1995). We can see from apparent H/C ratios that it decreased in runs with premixed decalin-catalyst compared to the base run (**Table 4.5**). I think that it is a clear sign of better upgrading in runs with decalin and catalyst mixture.

It was mentioned before that runs with additives resulted in higher combustion temperatures, as evident from graph of combustion front temperatures versus time in **Fig 4.33**. Adding decalin and catalyst increased significantly the combustion temperature. Difference between average temperatures of first and third runs is 130°C. Unfortunately,

there is no data on combustion temperature with time in the thesis of Palmer. I could compare only average temperatures of combustion to choose between hydrogen donors. Average combustion temperatures for decalin are higher than for tetralin as seen from **Table 4.5**.

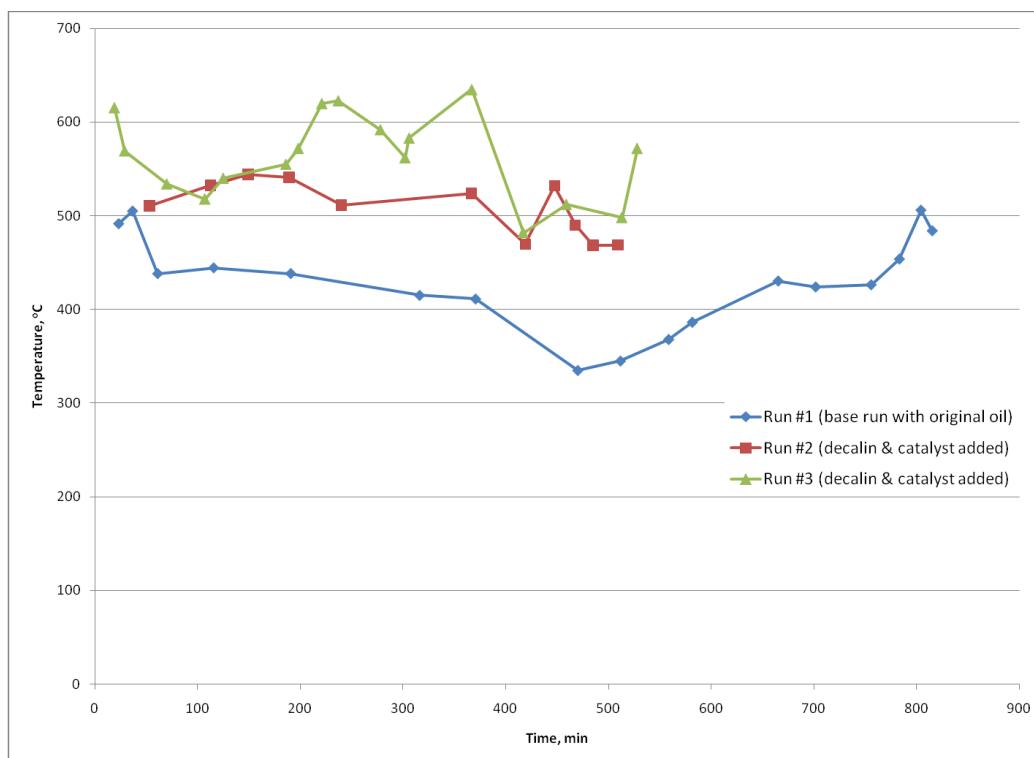


Fig. 4.33 – Combustion front temperatures for all runs.

Table 4.5 – Summary of experimental result.

	Run #1 (base run)	Run #2 (decalin + iron catalyst)	Run #3 (decalin + iron catalyst)	Run with tetralin + iron catalyst)
<i>m-ratio</i>	0.24	0.23	0.22	0.25
Average apparent H/C ratio	1.93	1.14	0.69	1.70
Median apparent H/C ratio	1.6	1	0.69	-
Average combustion temperature (°C)	430	508	563	492
Combustion front velocity (ft/hr)	0.19	0.32	0.31	0.46
Oil recovery (%)	81	88	88	86
API gravity at end of combustion run	10.5	12.5	14.3	15
*Average viscosity at end of combustion run (cp)	740	399	377	221**

* Oil viscosity averaged for the three temperatures: 40°, 50° and 60°C

** Based on Palmer (Palmer-Ikuku, 2009) oil viscosity in base run was 504cp.

5 SUMMARY, CONCLUSIONS, AND RECOMMENDATIONS

5.1 Summary

The main objective of my research is to experimentally evaluate oil upgrading and recovery during in situ combustion using a combination of hydrogen donor decalin and an organometallic catalyst. 10° API Gulf of Mexico heavy oil is used for the experiments. Decalin and tetralin's production enhancing abilities were compared by analyzing the experimental results with data from the thesis of Palmer.

Four in situ combustion runs were performed with a Gulf of Mexico heavy oil and three of them were successful. The first run was base a run made without any additives. Two runs were made with premixed decalin (5% by oil weight) and an organometallic catalyst (750 ppm). The same oil and catalyst were used in the for experiments of Palmer (Palmer-Ikuku, 2009), and the only difference was in the hydrogen donor type. Following conditions were kept constant during all experimental runs: air injection rate at 3.1 L/min and combustion tube outlet pressure at 300 psig.

5.2 Conclusions

Based on the experimental results, the following conclusions can be made:

1. Experimental results with decalin and organometallic catalyst showed an increase in oil recovery to 7%, increase in oil API gravity and higher velocity of combustion.
2. 2-3° API increase with decalin as hydrogen donor, similar to that for tetralin.

3. 381-402cp oil viscosity at the end of combustion run for the runs with decalin, compared to 768 cp to the base run. Similar oil upgrading effects were observed with tetralin as hydrogen donor.
4. Low temperature oxidation appears to occur during the base run. This is probably due to air bypassing the combustion front. The reason for it is not well understood. In experiments with additives this effect was less or did not happen at all.
5. Apparent H/C ratio is lower for runs with decalin-catalyst compared to the base run indicating upgrading of oil. Large apparent H/C ratio is a result of oxygen being consumed in LTO reactions, which do not produce carbon oxides. The viscosity and boiling range of the crude oil increases because of LTO.
6. The combustion temperature of decalin-catalyst run is higher compared to the base run, and this increase of temperature is very noticeable (up to 130°C). High combustion temperature prevents LTO during combustion process of oil premixed with decalin and catalyst.
7. There is a large variation of average combustion temperature even in runs with the same decalin-catalyst additive. The average temperature for the second run is 508°C while the average temperature for the third run is 563°C.
8. Oil recovery factors in both decalin-catalyst runs (88% OOIP) increased by 7% compared to the base run (81% OOIP).
9. Oil recovery factor for run with decalin is higher than that with tetralin by 2%. The fact that decalin half the price of tetralin, the use of decalin is preferred for enhanced in situ combustion.

10. Combustion time with decalin-catalyst decreased from 815 min (base run) to 495 min (run 2) and 527 min (run 3). It happens due to number of reasons, including lower viscosity of oil and higher temperature of combustion. Oil moves faster because of low viscosity and it leads to higher combustion front velocity. With high temperatures, heat can go further and preheat the oil. It starts movement of oil from zones which are not available at lower temperatures. This is significant result as in field run it means huge savings on working time of compressors and faster return of investments.
11. API gravity of produced oil increased in all combustion runs compared to the original oil. The gravity at the end of combustion in decalin-catalyst runs (12.5 °API and 14.3 °API in run 2 and 3 respectively) was higher in comparison to the base run (10.5°API). These runs confirm upgrading abilities of decalin and organometallic catalyst.
12. Water saturation of the sand mix used in combustion should be higher. During combustion, water from the reservoir evaporates and creates a steam front that moves towards the production well. This steam and hot water is an additional force that moves the oil to the producer. Presence of this force would have given even better results in oil production.

5.3 Recommendations

1. Investigate a way to disperse decalin and catalyst through the porous media previously saturated with oil and water, as in lab we premix it with oil, which is impossible in real life.

2. Investigate the economics of both decalin and decalin-catalyst for use in heavy oil recovery using in situ combustion.
3. Conduct in situ combustion experiments with decalin and catalyst using a sand pack with heterogeneities as found in the field.

REFERENCES

- Alboudwarej H, F.F., Taylor S, Badry R, Bremner C, Brough B, Skeates C, Baker a, Palmer D, Pattison K, Beshry M, Krawchuk P, Brown G, Calvo R, Cañas Triana Ja, Kundu D, Hathcock R, Koerner K, Hughes T, López De Cárdenas J and West C. 2006. Highlighting Heavy Oil *Oilfield Review* **18** (2): 34-53.
- Cristofari, J., Castanier, L.M., and Kovscek, A.R. 2008. Laboratory Investigation of the Effect of Solvent Injection on In-Situ Combustion. *SPE Journal* **13** (2): 153-163. 997. DOI: 10.2118/99752-pa
- Fassihi, M.R., Meyers, K.O., and Baslie, P.F. 1990. Low-Temperature Oxidation of Viscous Crude Oils. *SPE Reservoir Engineering* **5** (4): 609-616. 15648-PA. DOI: 10.2118/15648-pa
- He, B., Chen, Q., Castanier, L.M., and Kovscek, A.R. 2005. Improved In-Situ Combustion Performance with Metallic Salt Additives. Paper Society of Petroleum Engineers 93901-MS presented at the SPE Western Regional Meeting, Irvine, California, 03/30/2005.
- Mamora, D.D. and Brigham, W.E. 1995. The Effect of Low-Temperature Oxidation on the Fuel and Produced Oil During In-Situ Combustion of a Heavy Oil. *In Situ* **19** (4): 341-365.
- Mohammad, A.A.A. and Mamora, D.D. 2008. In Situ Upgrading of Heavy Oil under Steam Injection with Tetralin and Catalyst. Paper 2008, SPE/PS/CHOA International Thermal Operations and Heavy Oil Symposium 11760 presented at the International Thermal Operations and Heavy Oil Symposium, Calgary, Alberta, Canada, 10/20/2008.
- Nares, H.R., Schachat, P., Ramirez-Garnica, M.A., Cabrera, M., and Noe-Valencia, L. 2007. Heavy-Crude-Oil Upgrading with Transition Metals. Paper Society of Petroleum Engineers 107837-MS presented at the Latin American & Caribbean Petroleum Engineering Conference, Buenos Aires, Argentina, 04/15/2007.
- Ovalles, C.S., Vallejos, C., Vasquez, T., Rojas, I., Ehrman, U., Benitez, J.L. et al. 2003. Downhole Upgrading of Extra-Heavy Crude Oil Using Hydrogen Donors and Methane under Steam Injection Conditions. *Petroleum Science and Technology* **21** (1): 255 - 274.
- Palmer-Ikuku, E. 2009. Experimental Study of In Situ Combustion with Tetralin and Metallic Catalysts. Master of Science, Texas A&M University, College Station.
- Ramirez-Garnica, M.A., Mamora, D.D., Nares, R., Schacht-Hernandez, P., Mohammad, A.A.A., and Cabrera, M. 2007. Increase Heavy-Oil Production in Combustion Tube Experiments through the Use of Catalyst. Paper Society of Petroleum

- Engineers 107946-MS presented at the Latin American & Caribbean Petroleum Engineering Conference, Buenos Aires, Argentina, 04/15/2007.
- Ramirez-Garnica, M.A., Perez, J.R.H., Cabrera-Reyes, M.D.C., Schacht-Hernandez, P., and Mamora, D.D. 2008. Increase Oil Recovery of Heavy Oil in Combustion Tube Using a New Catalyst Based on Nickel Ionic Solution. Paper 2008, SPE/PS/CHOA International Thermal Operations and Heavy Oil Symposium 117713-MS presented at the International Thermal Operations and Heavy Oil Symposium, Calgary, Alberta, Canada, 10/20/2008.
- Wu, C.H. and Fulton, P.F. 1971. Experimental Simulation of the Zones Preceding the Combustion Front of an In-Situ Combustion Process. **11** (1): 38-46. 2816-PA. DOI: 10.2118/2816-pa
- Zhong, L.G., Liu, Y.J., Fan, H.F., and Jiang, S.J. 2003. Liaohe Extra-Heavy Crude Oil Underground Aquathermolytic Treatments Using Catalyst and Hydrogen Donors under Steam Injection Conditions. Paper Society of Petroleum Engineers 8486 presented at the SPE International Improved Oil Recovery Conference in Asia Pacific, Kuala Lumpur, Malaysia, 10/20/2003.

VITA

Name: Dauren Mateshov

Permanent address: 3116 TAMU, Richardson Building
Texas A&M University, College Station, Texas, 77843

Education: B.S. Petroleum Engineering
Kazakh-British Technical University, Kazakhstan 2007
M.S. Petroleum Engineering
Texas A&M University, College Station 2010

Member: Society of Petroleum Engineers

Email address: dmateshov@gmail.com